Aalto University
School of Chemical
Technology

School of Chemical Technology
Degree Programme of Environomical Pathways for Sustainable Energy Systems

Ajimufti Azhari

HYDROGEN PRODUCTION VIA REFORMING OF PYROLYSIS OIL AQUEOUS FRACTION

Master's thesis for degree of Master of Science in Technology submitted for inspection, Espoo, 01 August 2014.

Supervisor **Professor Juha Lehtonen**

Instructor **Ville Paasikallio, M.Sc. (Tech)**

Aalto University
School of Chemical
Technology

Aalto University, P.O. BOX 11000, 00076 AALTO
www.aalto.fi

Abstract of master's thesis

Author Ajimufti Azhari

Title of thesis Hydrogen Production via Reforming of Pyrolysis Oil Aqueous Fraction

Department Biotechnology and Chemical Technology

Professorship Industrial Chemistry **Code of professorship** KEM-40

Thesis supervisor Juha Lehtonen

Thesis advisor(s) / Thesis examiner(s) Ville Paasikallio, M.Sc. (Tech)

Date 01.08.2014 **Number of pages** 68+19 **Language** English

Abstract

Increase in energy demands and the need of new and renewable energy sources pushes the development of biomass utilization. One of the new emerging interests is hydrogen production from pyrolysis oil aqueous fraction using catalytic steam reforming. Although it is known firstly as a source of valuable chemicals and sugars, hydrogen production via reforming is indicated to be the most cost-effective way for utilizing pyrolysis oil aqueous fraction. The literature review revealed that wide range of catalysts and process conditions have been tested and main challenges revolved around catalyst stability, feeding system and reactor design. Based on the stability issue, oxidative steam reforming and testing of different types and combinations of reforming catalysts was chosen as a topic of the experimental part master's thesis.

In the experimental part, oxidative steam reforming of pyrolysis oil aqueous fraction from condenser unit in fast pyrolysis of forest thinning was tested using three different catalysts and catalyst combination and four different oxygen concentrations —represented by different O/C ratios. The experiments were carried out in a fixed bed steel reactor with process conditions set up as reaction temperature of 650^{o}C, atmospheric pressure and S/C of 3.84. It was found that combination of zirconia monolith as pre-reformer and commercial nickel catalyst (Reformax) to be the best catalyst combination that enhanced the stability of carbon-to-gas conversions and hydrogen production. With this combination, the carbon-to-gas conversions remained above 80% for 4 hours and hydrogen productions above 70% in any O/C ratio used. This catalyst combination also showed role in suppressing the rate of C2 formation side reactions. It was also found that increase of oxygen fed into in the system benefited to create more stable carbon-to-gas conversions and hydrogen production profiles. The observed main problem with the experiments was carbon coking at the top of the reactor as a result of feed depolymerisation and decomposition during the spraying process.

Keywords pyrolysis oil, aqueous fraction, oxidative steam reforming, hydrogen

Forewords

The author of this thesis would like to thank people who has been supporting and helping throughout the completion of this master's thesis.

1. VTT Technical Research Centre of Finland, where all the experiment were conducted and for the funding support
2. Pekka Simell, supervisor from VTT for offering the opportunity also for guiding through administration, practical and work related matters
3. Juha Lehtonen, supervisor from Aalto University for his guidance, feedbacks and insightful opinions
4. Ville Paasikallio, instructor from VTT for patiently guiding during the experiment as well as giving comments and feedbacks during the writing of this thesis
5. Katja Heiskanen, Mari-Leena Koskinen-Soivi, Johanna Kihlman, and Kaija Luomanperä from VTT who were wonderfully guiding through laboratory adaptation and always ready for practical helps
6. SELECT Program and KIC InnoEnergy for providing great learning experiences and study grants
7. Friends and family for their endless supports and powerful discussions

This master's thesis was carried out from February 2014 until July 2014. The author hopes that this master's thesis will be a small useful puzzle for development of biorefinery industry.

Espoo, 4 July 2014

Author,

Ajimufti Azhari

Contents

Abbreviations

ATR	Autothermal Reforming
C2	Refers to a molecule with 2 carbons
C2G	Carbon-to-gas
CHP	Combined Heat and Power
GC	Gas chromatograph
HHV	High heating value
NREL	National Renewable Energy Laboratory
NTP	Normal Temperature and Pressure
OSR	Oxidative Steam Reforming
O/C	Oxygen-to-carbon ratio
POX	Partial Oxidation
S/C	Steam-to-carbon ratio
SR	Steam Reforming
vol-%	Volume percentage
VTT	Valtion Teknillinen Tutkimuskeskus/ Technical Research Centre of Finland
WHSV	Weight hourly space velocity
wt-%	Weight percentage

1. Introduction

Increase in population that corresponds to increase in energy demand has been a critical challenge for the world. This situation has pushed new and renewable energy technologies to be developed and applied in recent years. One of the options is to utilize biomass, especially biomass waste and lignocellulosic biomass since it accounts for zero anthropogenic carbon accumulation and does not compete with food production. Thermochemical conversion processes are by far the most promising technologies to convert these types of biomass [1, 2, 3]. Pyrolysis is one technology that is proven to convert biomass into more energy densified, versatile and easy to transport pyrolysis oil. However, further refining of this product is needed to make it more competitive in the market.

Many pathways have been proposed to improve the utilization pyrolysis oil, ranging from generating electricity directly to conversion of pyrolysis oil into biofuels and chemicals via upgrading [2]. Moreover, to increase the efficiency of the pyrolysis system, the aqueous fraction of pyrolysis oil—which has been by far considered as waste stream—is now being investigated as source of valuable chemicals, sugars and also to be a good source of hydrogen via catalytic steam reforming [4, 5, 6].

This thesis work is divided into two main parts: literature review and experimental part. The literature review provides background information regarding current technologies used for oxidative steam reforming of pyrolysis oil aqueous fraction, to be a guideline in setting up the experimental conditions. The objectives of the work are to find the best catalyst from some commercial and in-house made catalyst options for hydrogen production and also to investigate the effect of oxygen addition to the stability of the catalytic system. One commercial catalyst and two in-house made catalysts are being investigated

under four different oxygen concentrations in the feed. Other parameters are taken from available literature works to be implemented directly to the system configurations.

The work also includes discussion and calculation of several important figures such as carbon balance of the process and effects of each variable to the product concentration profiles as a function of time-on-stream. Moreover, several interesting phenomena that are found during the experiment will also be discussed.

2. Pyrolysis

Pyrolysis is one type of thermochemical conversion process of carbon containing feedstock, which is generally known as thermal decomposition occurring under inert or non-oxidative environment [2, 3]. In general, pyrolysis of biomass can be represented as the following reaction.

$$C_nH_mO_p(\text{biomass}) \xrightarrow{heat} \sum_{liquid} C_aH_bO_c + \sum_{gas} C_dH_eO_f + H_2O + \text{C (char)} \qquad (1)$$

Pyrolysis can be operated within different temperature range, heating rates and residence times. These different modes will result in different product distributions, generally between solid, liquid, and gas proportions. Table 1 shows several common pyrolysis (and gasification for comparison) modes. Note that in gasification oxygen or steam is used to promote partial oxidation.

TABLE 1 Typical product yields of different modes of thermochemical treatment [1]

Mode	Conditions	Liquid (%-wt)	Solid (%-wt)	Gas (%-wt)
Fast pyrolysis	~500°C, short hot vapor residence time (~1 second)	75	12	13
Intermediate	~500°C, intermediate hot vapor residence time (~10-30 seconds)	50	25	25
Slow-torrefaction	~290°C, solids residence time ~30 min	-	82	18
Slow-carbonization	~400°C, long vapor residence time (~hours-days)	30	35	35
Gasification	~800°C	5	10	85

Nowadays, fast pyrolysis process is of particular interests since its major product is the liquid fraction, which is easy to transport, store and further process. From Table I, it can be seen that temperature and residence time have important roles in product composition. Higher temperature will increase gas production while lower temperature tends to give higher solid fraction. On the other hand, longer residence time will allow more secondary reactions to happen, resulting in higher gas yield.

2.1 Fast Pyrolysis of Biomass

Applying high temperature in a very short exposure time to biomass will decompose the material mostly into vapours and aerosols with some char and gas. This is the main concept of fast pyrolysis of biomass. After cooling and condensation, the vapours can be collected in the form of dark brown liquid, which is called pyrolysis oil or bio-oil. There are several main features of fast pyrolysis process which are required to increase the liquid yield, which are [2, 3]:

- Very high heating rate and heat transfer is required due to low thermal conductivity of biomass. The biomass is usually ground into fine particles (< 3 mm) to ensure the heat transfer to occur effectively.
- Tightly controlled temperature (around 500^{o}C) to ensure the highest liquid yield of biomass. Note that higher temperature will produce more gas fraction while lower temperature will create more solid product.
- Very short residence time (< 2s) to minimize secondary reactions
- Rapid removal of product char to minimize vapour cracking
- Rapid quenching of pyrolysis vapours to produce pyrolysis oil

Despite the fact that any form of biomass can be used, wood is commonly preferred as the main feedstock for fast pyrolysis process. Wood has big advantages in low ash content, product consistency and repeatability [2]. Disregarding the feedstock being used, commercial pyrolysis process usually contains three main stages [2]:

- Feed system: reception, storage, handling, preparation and pre-treatment
- Main system: conversion of biomass by fast pyrolysis mostly into liquid bio-oil
- Product collection system

Additionally, downstream processing (i.e. converting bio-oil into refining or to another marketable end-product such as electricity, heat, biofuels and/or chemicals) can also be part of more advanced plants.

Growing interest on catalytic pyrolysis process also takes place nowadays. The idea of catalytic pyrolysis is to upgrade the product of pyrolysis before the condensation process, which means introducing the catalyst into the system to convert the pyrolysis vapours into more desired hydrocarbon products. It can be done by placing the catalyst directly as bed materials in the fluidized pyrolysis reactor or by adding a separate reactor to the downstream; a fluidized pyrolyzer with inert bed material followed by a fixed-bed or fluidized-bed reactor with catalyst bed in it. However, the vapours can be sometimes condensed first into pyrolysis oil before being fed into the second reactors. Zeolites and mesoporous materials have been used widely as catalyst to decrease oxygen content in the product [14]. The aim of catalytic pyrolysis process is to avoid further severe upgrading steps of pyrolysis product, especially regarding oxygen content in the product.

2.2 Products of Pyrolysis

As mentioned briefly before, in principle three types of products are obtained from pyrolysis [2, 3].

- *Solid:* The solid product of pyrolysis is known as char. It contains roughly 85% of carbon with some oxygen, hydrogen and inorganic ash.
- *Liquid:* Liquid fraction called bio-oil is the main product of fast pyrolysis. It is a black tarry fluid containing mixture of oxygenated hydrocarbons and water (up to 30%).
- *Gas:* Gas fraction contains non-condensable gas from the primary decomposition. Additionally, some non-condensable can be formed due to secondary cracking of vapours, which is usually referred to secondary gases.

As the main product aimed from fast pyrolysis is the liquid fraction, gases and chars are considered as by-products, which contain around 30% of energy content of the feed material [2]. The liquid is composed of very complex mixture of oxygenated hydrocarbons with significant amount of water, both from the feed and from reactions during the pyrolysis [2, 3]. Table 2 shows the typical physicochemical properties of crude pyrolysis oil from wood.

TABLE 2 Typical properties of wood-derived crude pyrolysis oil [2]

Physical property	**Typical value**
Moisture content	25%
pH	2.5
Specific gravity	1.20
Elemental composition (db.)	
C	56 wt-%
H	6 wt-%
O	38 wt-%
N	0-0.1 wt-%
HHV (as produced)	17 MJ/kg
Viscosity (40^{o}C with 25% water)	40-100 mpa s
Solids (char)	0.1%-wt
Vacuum distillation residue	up to 50%

Many pathways have been established and developed to upgrade the quality of pyrolysis oil. These actions are needed to overcome such issues of pyrolysis oil as poor stability (aging), complex nature and other undesired characteristics. The challenging properties of pyrolysis oil include low pH, low heating value, poor volatility, high viscosity and high oxygen content [15]. Figure 1 shows various options in bio-oil upgrading into more common end-products. Besides upgraded into more competitive products, pyrolysis oil can be also utilized directly as fuel to generate heat and/or electricity.

As mentioned in the previous section, catalytic pyrolysis is also a way to improve the pyrolysis oil quality. Catalytic process is believed to provide less complicated and more integrated pathway to improve pyrolysis oil quality before condensation takes place. The idea of upgrading the product while it is still in

vapour phase can be achieved due to several reactions involved on the catalyst surface: dehydration, decarboxylation and decarbonylation, which deoxygenate the feed. Some other reactions included are cracking, polymerization and aromatization [6, 14].

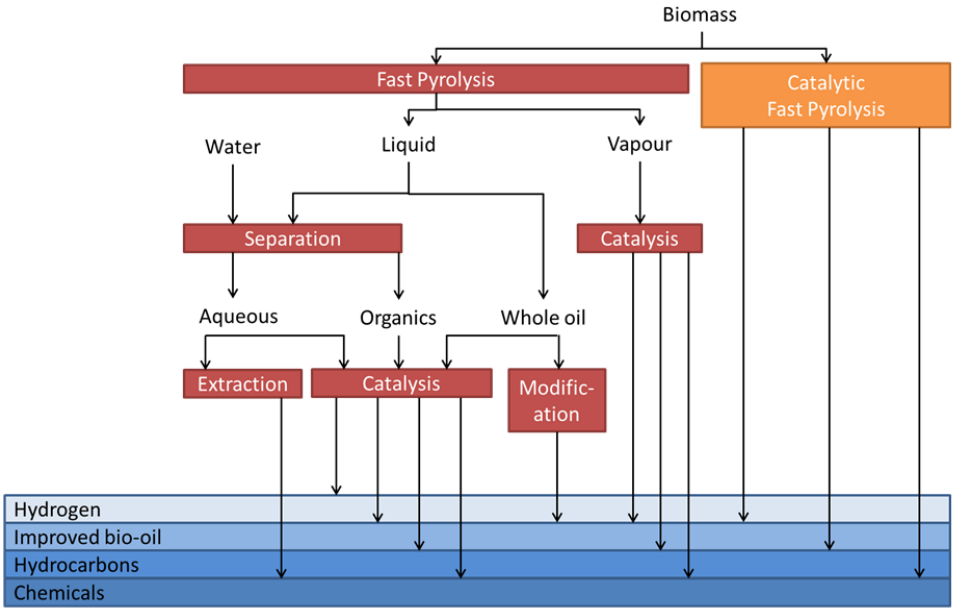

FIGURE 1 Overview of fast pyrolysis upgrading methods [2]

In comparison with conventional fast pyrolysis, catalytic pyrolysis results in lower yield of pyrolysis oil due to several reasons. Aho et al. [14, 16] reported that introduction of catalyst to pyrolysis system promoted higher coke formation on the surface of the catalyst and more gases containing carbon (CO and CO_2) are formed due to the upgrading reactions involved. Moreover, water yield is also increased upon addition of catalyst to the process. The more catalyst is used in the system, the more significant the changing is with the respective effects.

2.2.1 Pyrolysis Oil Aqueous Fraction

Another important step of pyrolysis oil utilization is by phase separation process in which aqueous phase of the oil is separated from the whole oil fraction.

Pyrolysis oil contains a considerable amount of water, up to 15-30%-wt for wood [9, 10] and 36-45%-wt for straw and hay [11]. The separation cannot be done by distillation due to complex chemistry and instability of bio-oil [7]. Thus, several other methods are proposed and the cheapest method known is water solvent extraction [7, 8]. Using this method, water is added directly into pyrolysis oil until it reaches certain limit (typically 30-45%-wt [12]) after which it forms two separable layers. The aqueous top layer consists mainly of water-soluble polar-carbohydrate-derived compounds while the oily bottom layer is rich in less-polar lignin-derived (mainly) aromatic compounds [6].

The aqueous fraction of pyrolysis oil is known to be a good feedstock for isolating several valuable chemicals such as sugar compounds and acetic acid [7]. The separation treatment was considered firstly to recover valuable oxygenated compounds [4, 5, 6], before bio-oil is converted transportation fuels mostly via catalytic upgrading. However, due to very low concentration of the valuable compounds in the aqueous phase, the separation becomes very costly and not economically interesting [13]. Nowadays, there is growing interest in hydrogen production via catalytic reforming of pyrolysis oil aqueous fraction, which is favourable due to utilization of the whole fraction and relatively known and established methods.

As for catalytic pyrolysis, more water is produced during the reactions, resulting in higher water content of the product. Usually there is no additional water needed to separate the aqueous fractions and the oil fractions. There are not many researches about the difference between each aqueous phase compositions coming from non-catalytic and catalytic pyrolysis process. However, there is an indication that different types of sugars can be obtained with catalytic pyrolysis: for instance different levoglucosan concentrations can be obtained with different type of catalysts [14].

3. Oxidative Steam Reforming

Hydrogen is mainly produced via reforming reactions, in which hydrocarbon is being reformed to produce hydrogen and other side products such as CO or CO_2. The reforming process is usually carried out catalytically using either steam (steam reforming) or oxygen (partial oxidation) to break the hydrocarbon compounds into H_2-rich gas as its product outlet.

Steam reforming (SR) is known as catalytic process giving the highest yield of produced hydrogen [17, 22]. In this process, no air/oxygen is allowed to be in the system, thus preventing combustion of desired components. Despite being the most productive method, highly endothermic SR requires an external heat source. Meanwhile, partial oxidation (POX) is another route to produce hydrogen via introduction of limited combustion in catalytic system. POX involves just enough oxygen in the feed to convert carbon in the fuel into carbon monoxide in a very short residence time [22].

Another reforming option is to feed both steam and oxygen together into the system, which is commonly referred to as oxidative steam reforming (OSR) [17]. The general equation for OSR can be expressed by the following Eq. (1).

$$C_nH_mO_p + aO_2 + \mathrm{b}H_2O \rightarrow \mathrm{c}H_2 + dCO_2 \quad (1)$$

As a combination of POX and SR, OSR utilizes the heat generated from exothermic POX reactions to support the endothermic reactions in SR. When the heat from the POX reactions thermally balances the endothermic reactions of SR, the total reactions of OSR become thermoneutral. Reforming in these conditions is called autothermal reforming (ATR), which is a special case of OSR and has different unique process conditions for different fuels used [17]. Comparisons of these three methods applied for hydrogen production can be seen in Table 3.

TABLE 3 Summarized comparisons between three reforming options to produce hydrogen: SR, ATR (as part of OSR) and POX [17, 22, 40]

Characteristics	**Steam Reforming**		**Autothermal Reforming**		**Partial Oxidation**	
Overall enthalpy	Endothermic (64 to 310 kJ/mol)		Thermoneutral (~0 kJ/mol)		Exothermic (-778 to 71 kJ/mol)	
System volume	Complex reactor and heat integration makes SR system tends to be large and heavy.		Less heat integration and reactor complexity makes ATR needs less volume.		Lower system volume due to fast reaction time and less heat integration.	
	Steam Reforming		**Autothermal Reforming**		**Partial Oxidation**	
	Advantages	**Disadvantages**	**Advantages**	**Disadvantages**	**Advantages**	**Disadvantages**
Hydrogen yield	Mostly >50% at T > 600^{o}C and S/C=1	-	Around 50%	Lower hydrogen yield compared to SR	-	Relatively low yield
Heat requirement	-	External heat required	Ideally does not require external energy	Needs start-up heat and control systems.	No external heat required (exothermic)	Needs heat removal system.
Start-up	Relatively stable during transition operation	Needs external igniter. Slow start-up due to high volume and limited heat transfer efficiency.	Moderate response time. Response time depends on POX portion of the whole system when switching from ATR to POX.	Transient fluctuations may occur at rate where it might affect switching efficiency.	Fast start-up and easy to control.	High temperature start-up and shutdowns might cause catalyst degradation

Despite the advantages it provides, ATR conditions are hard to be achieved due to limitations in heat management (e.g. heat losses) in industrial scale processes [1]. There are several ways to compensate these heat losses, where the most common way is to add more oxygen to increase oxygen-to-carbon (O/C) ratio. Several experiments suggested that the optimal operating condition for methane OSR is to be O/C = 0.7 – 1.0 and steam-to-carbon ratio (S/C) = 1.5 – 2.0, with temperatures between 700-800^{o}C [18, 19].

3.1 Chemistry and Thermodynamics of Oxidative Steam Reforming

The chemistry and thermodynamics of OSR has been reviewed and investigated by using different feedstock and model compounds. This section will provide detailed information regarding both matters in a general review.

3.1.1 Involved Reactions

OSR consists of a complex network of consecutive/competitive reactions. Each reaction has its own intrinsic characteristics in terms of kinetics, which is affected by the selection of catalyst and reaction conditions. Several key reactions are listed below [17].

Steam Reforming

$$C_nH_mO_p + H_2O \rightarrow H_2 + CO \tag{2}$$

Water-gas Shift

$$CO + H_2O \leftrightarrow H_2 + CO_2 \qquad \Delta H^o_{298} = -41kJ/mol \tag{3}$$

Partial Oxidation

$$C_nH_mO_p + \frac{n}{2}O_2 \rightarrow H_2 + CO \tag{4}$$

Complete Oxidation

$$C_nH_mO_p + O_2 \rightarrow H_2O + CO_2 \tag{5}$$

Incomplete Oxidation

$$C_nH_mO_p + O_2 \rightarrow H_2O + CO \tag{6}$$

$$C_nH_mO_p + O_2 \rightarrow H_2 + CO_2 \tag{7}$$

Dry Reforming

$$C_nH_mO_p + CO_2 \rightarrow H_2 + CO \tag{8}$$

For hydrogen production purpose, the main reactions of OSR consist of steam reforming, partial oxidation and water gas shift reactions, which directly produce hydrogen. However, oxidation reactions are also desired mainly as heat producer to support the endothermic main reactions.

Beside the list of hydrogen and carbon monoxide producing reactions, there are also several side reactions which are undesirable due to consumption of desired products or production of undesired products such as carbon. Carbon accumulation might lead to coking problem in the catalyst (leading to deactivation), hot spots in the reactor, uneven heat transfer and flow blocking [17]. Those reactions are listed below.

Hydrogen Oxidation

$$H_2 + O_2 \leftrightarrow H_2O \qquad \Delta H^o_{298} = -286kJ/mol \tag{9}$$

Carbon Monoxide Oxidation

$$CO + O_2 \leftrightarrow CO_2 \qquad \Delta H^o_{298} = -283kJ/mol \tag{10}$$

Methanation

$$C + 2H_2 \leftrightarrow CH_4 \qquad \Delta H^o_{298} = -75kJ/mol \tag{11}$$

$$CO + 3H_2 \leftrightarrow CH_4 + H_2O \qquad \Delta H^o_{298} = -217kJ/mol \tag{12}$$

$$CO_2 + 4H_2 \leftrightarrow CH_4 + 2H_2O \qquad \Delta H^o_{298} = -178kJ/mol \tag{13}$$

Reverse Water-gas Shift

$$CO_2 + H_2 \leftrightarrow CO + H_2O \qquad \Delta H^o_{298} = 41kJ/mol \tag{14}$$

Decomposition

$$C_nH_m \rightarrow nC + \frac{m}{2}H_2 \tag{15}$$

Boudouard

$$2CO \leftrightarrow C + CO_2 \qquad \Delta H^o_{298} = 162kJ/mol \qquad (16)$$

CO and CO_2 Hydrogenation

$$CO + H_2 \leftrightarrow C + H_2O \qquad \Delta H^o_{298} = -131kJ/mol \qquad (17)$$

$$CO_2 + 2H_2 \leftrightarrow C + 2H_2O \qquad \Delta H^o_{298} = -90kJ/mol \qquad (18)$$

Note that in hydrogen production, some of these side reactions might also benefit the whole system. For example, carbon monoxide oxidation is desirable for hydrogen production since it is easier to separate CO_2 in gas purification (if applicable).

3.1.2 Effect of Temperature

As all reaction rates and chemical equilibrium are heavily dependent on the temperature, effect of this parameter is highly noticeable in the product composition. For oxidative steam reforming, hydrogen production will significantly increase in line with the raise in temperature. At certain point where reverse water-gas shift reaction takes over the system, the H_2/CO ratio will decrease with elevating temperature.

Based on the chemical equilibrium calculations presented in Figure 2, different feedstock has different optimum temperature to achieve highest hydrogen yield. It can be seen that longer chain or non-oxygenated hydrocarbon (Fig. 2a, methane, compared to 2b, diesel) requires lower reaction temperature to achieve the highest hydrogen yield while oxygenated hydrocarbon (Fig. 2c, methanol) has even lower temperature to produce the highest hydrogen yield.

Another phenomenon that can be seen from Figure 2 is the solid carbon formation. It is indicated in the picture that length of hydrocarbon chain has impact in carbon formation temperature range, longer chain hydrocarbon having

wider temperature range of carbon formation. Note that carbon formation still can occur and hard to predict based on thermodynamics at temperature above 150°C [17]

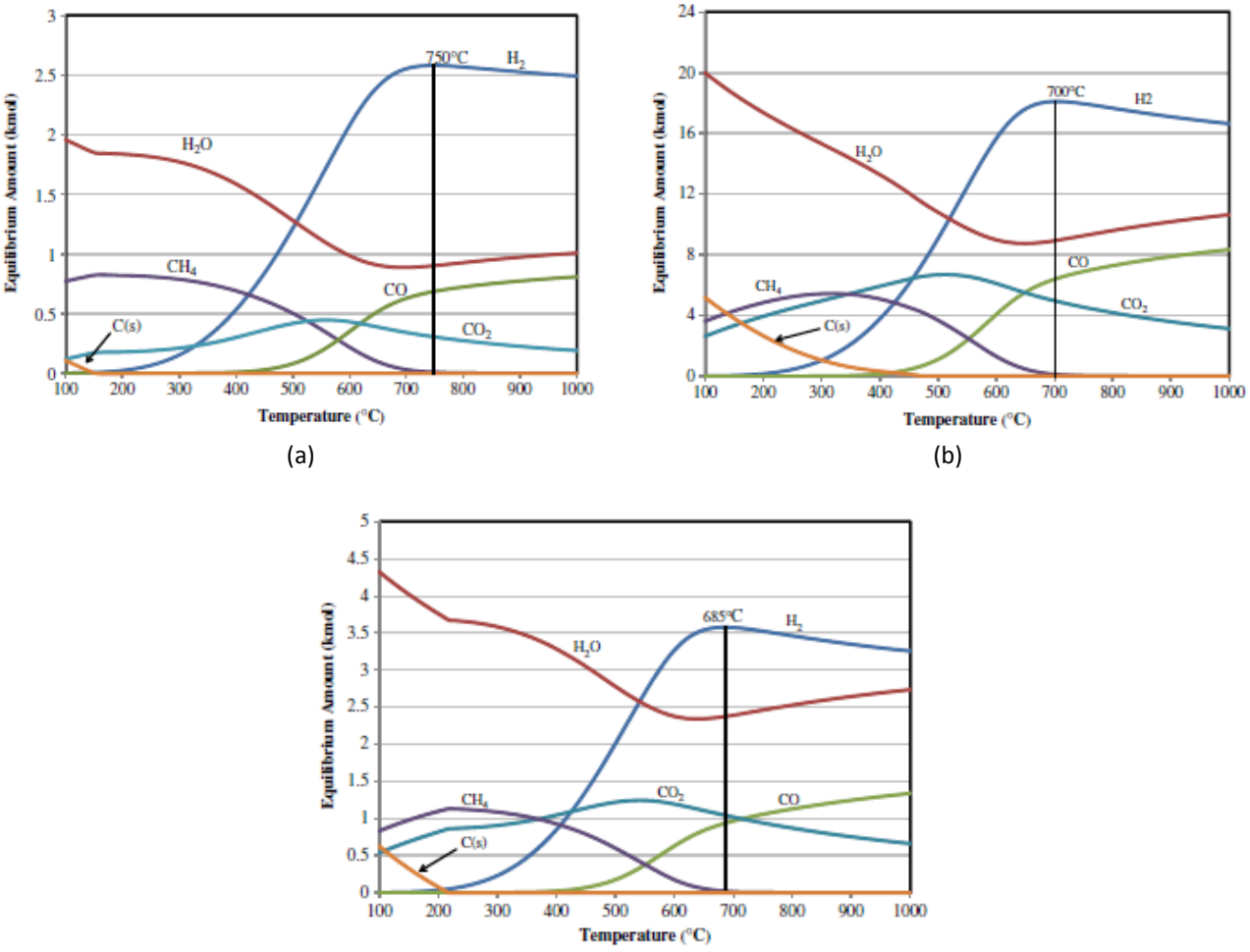

(a) (b)

(c)

FIGURE 2 Effects of temperature on product composition for OSR of 1 kmol (a) CH_4 (b) surrogate diesel mixture (40%-wt n-tetradecane, 40%-wt decaline, and 20%-wt 1-methylnapthalene) with average molecular formula for mixture is $C_{11.5}H_{20.7}$ (c) C_2H_5OH. All reforming were investigated at O/C = 0.7 (without accounting any O compound in the fuel), S/C = 1.5, and 0.1 MPa. All products are gases except C(s) and based on chemical equilibrium [17]

3.1.3 Effect of Oxidant

Effect of oxidant amount is usually indicated in terms of oxidant-to-fuel ratios. In OSR, there are two oxidants being used, which are oxygen (pure or in form of air) and steam. Thus, there are two ratios mostly being investigated: oxygen-to-

carbon ratio (O/C) and steam-to-carbon ratio (S/C). Figure 3 shows the effects of both oxidant-to-fuel ratios to amount of desired product of H_2 and CO.

As seen in Figure 3, both O/C and S/C have impact on product selectivity. As increase of O/C is introduced, the result shows a decline in selectivity towards H_2 and CO. It happens mainly due to promotion of oxidation and partial oxidation reactions. As sufficient amount of O_2 is introduced, more H_2 and CO is further converted into H_2O and CO_2. Further increase of O/C ratio will lead to conditions of stoichiometric combustion [17].

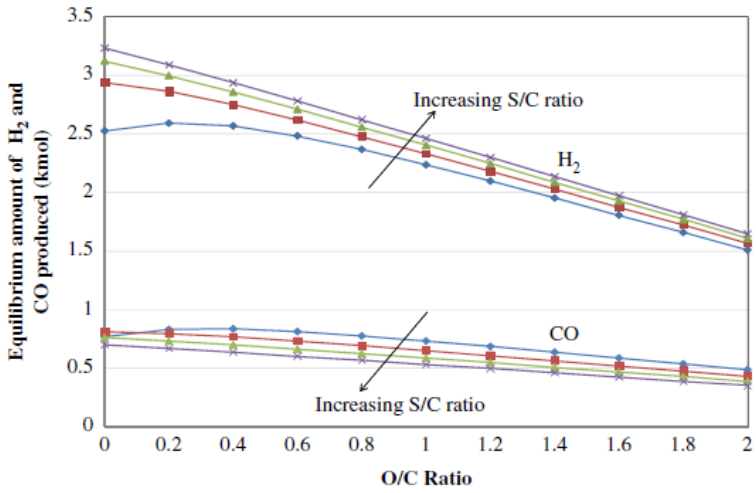

FIGURE 3 Effects of O/C and S/C ratios on H_2 and CO products (dry basis) from OSR of 1 kmol CH_4 at 800°C and 0.1 MPa (blue) S/C ¼ 1;(red) S/C¼ 1.5; (green) S/C¼ 2.0; (purple) S/C ¼2.5 (Equilibrium calculations performedby HSC Chemistry v6.12) [17].

On the other hand, increase of S/C results in increase of H_2 formation and decrease of CO concentrations. This result can be explained by the increase in steam reforming reaction due to addition of more steam into the system. Furthermore, the additional steam will also increase water-gas shift reaction which promotes formation of H_2 and decreases CO concentration. The same result trends are found for heavier hydrocarbon fuels [17].

At certain ratio of oxidants, dependent on type of fuel as well, autothermal operations (ATR) can be achieved. Ahmed and Krumpelt [4] develop a method to estimate the O/C and S/C ratios for ATR operation using the generalized Eq. (1). The maximum amount of H_2 obtained from the overall reaction is as shown by the expression below, assuming the steam is introduced to the system with stoichiometric amount to convert all carbon containing species into CO_2.

TABLE 4 Calculated thermoneutral (ATR) O_2 stoichiometric coefficient (a_o) for several hydrocarbon fuels [17, 20, 21]

Fuel	$\Delta \boldsymbol{H}_{\boldsymbol{f,fuel}}$ (kJ/mol)	ATR O_2 stoichiometric coefficient ($\boldsymbol{a_o}$)
Methanol, CH_3OH (l)	-238.9	0.23
Methane, CH_4 (g)	-74.9	0.44
Acetic acid, $C_2H_4O_2$ (l)	-487.0	0.47
Ethane, C_2H_6 (g)	-84.5	0.77
Ethylene glycol, C_2H_6OH (l)	-454.4	0.41
Ethanol, C_2H_6OH (l)	-277.0	0.61
Pentene, C_5H_{10} (g)	-20.9	1.59
Pentane, C_5H_{12} (g)	-146.4	1.87
Cyclohexane, C_6H_{12} (l)	-156.1	2.14
Benzene, C_6H_6 (l)	48.9	1.78
Toluene, C_7H_8 (l)	12.1	2.16
Iso-octane, C_8H_{18} (l)	-259.4	2.93
Gasoline, $C_{7.3}H_{14.8}O_{0.1}$ (l)	-221.7	2.61
n-Tetradecane, $C_{14}H_{30}$(l)	-403.7	5.07
n-Hexadecane, $C_{16}H_{34}$ (l)	-456.9	5.78
Diesel, $C_{16.2}H_{30.6}$ (l)	-426.3	5.79

$$C_nH_mO_p + aO_2 + (2n - 2a - p)H_2O \rightarrow (2n - 2a - p + \frac{m}{2})H_2 + nCO_2 \qquad (19)$$

Thus, based on Eq. (19), the maximum amount of hydrogen that can be produced is $(2n - 2a - p + \frac{m}{2})$. It can be seen that oxygen is the only species that negating the hydrogen yield from the entire system due to its ability to oxidize hydrogen and carbon species. However, it is good to notice that small portion of combustion is desired in ATR process to produce heat that will support the endothermic reforming reactions. The reaction enthalpy for Eq. (19) can be calculated as follows:

$$\Delta H_r = n\Delta H_{f,CO_2} - (2n - 2a - p)\Delta H_{f,H_2O} - \Delta H_{f,fuel} \quad (20)$$

To achieve ATR, $\Delta H_r = 0$. Rearranging Eq to obtain stoichiometric a for O_2 coefficient leads to

$$a_o = n - \frac{p}{2} + \frac{1}{2}\left[\frac{\Delta H_{f,fuel} - n\Delta H_{f,CO_2}}{\Delta H_{f,H_2O}}\right] \quad (21)$$

Values of a_o for various fuels have been estimated by several authors [17, 20, 21] with this method and the values can be seen in Table 5.

This a value can also indicate the energy requirement of the reactions in general. Different a value for specific reaction will change its reaction enthalpy. The formulation of different modes of operation [17] is concluded in Eq. (22).

$$a = \begin{cases} 0 & \text{Steam reforming} \\ n - \frac{p}{2} + \frac{1}{2}\left[\frac{\Delta H_{f,fuel} - n\Delta H_{f,CO_2}}{\Delta H_{f,H_2O}}\right] & \text{Thermoneutral} \\ n - \frac{p}{2} & \text{Partial Oxidation} \\ n + \frac{m}{4} - \frac{p}{2} & \text{Combustion} \end{cases} \quad (22)$$

Using the Eq. (20), Haynes and Shekhawat [17] plotted the changes in reaction enthalpies for several hydrocarbons as the function of O/C ratio, which is shown in Figure 3. From Table 5, it is discovered that the higher the C number of the fuel, the higher the thermoneutral coefficient will be. However, the corresponding O/C ratio to achieve ATR condition is roughly the same for all the species [17].

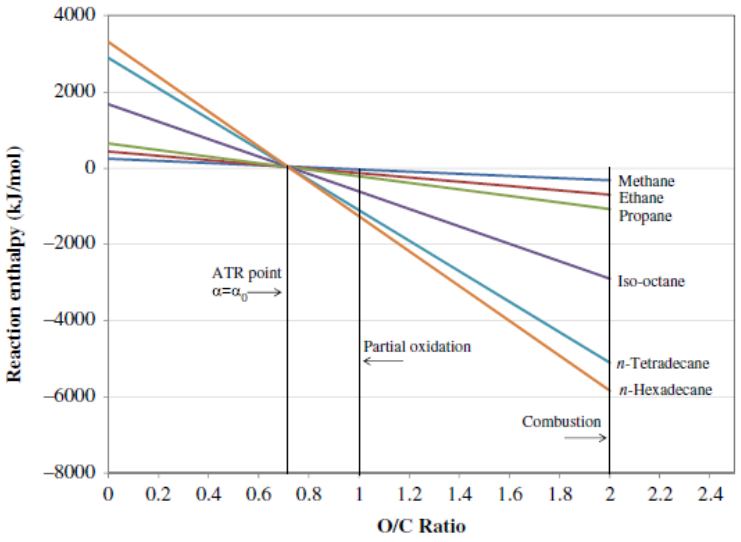

FIGURE 4 Enthalpy change (assuming product water as liquid) as function of O/C ratio for ATR of various hydrocarbon fuels [17]

Figure 4 also indicates that the reaction has the most energy intensive state when the a-value is set to 0 (O/C = 0), where the reaction becomes totally endothermic. In this state, only steam reforming takes place and external heat is needed to support the reaction. Despite being the most energy intensive, this configuration produces the most hydrogen as can be seen in Figure 2. Increasing a-value results in lowering the external heat needed for the reactions, until the thermoneutral point ($a = a_o$) is reached. This configuration of ATR is considered as the most energy efficient due to its ability to produce the highest hydrogen yield without any external energy required [17]. Exceeding the ATR point, the reaction enthalpy becomes exothermic and POX will take place. As even more oxygen being supplied, complete combustion will occur.

3.1.4 Effect of Pressure

As the overall reactions of OSR include a volume expansion, where the number of product moles is higher than reactant moles, lower pressures are favoured thermodynamically. Production of H_2 will decrease upon increase in operating

pressure, as well as CO, due to the limitations of equilibrium of steam reforming at higher pressure [17]. The effect of pressure is visually shown on Figure 5.

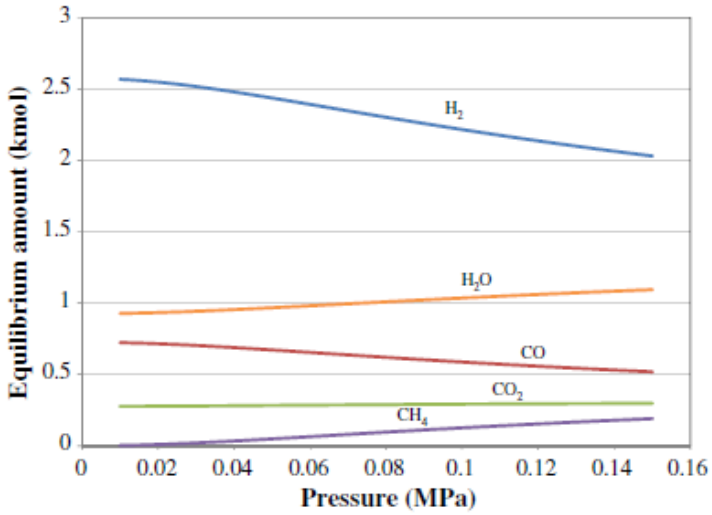

FIGURE 5 Equilibrium product distribution as a function of pressure for the OSR of 1 kmol CH_4 (O/C=0.7, S/C=1.5 and 800^{o}C) [17]

3.2 Catalyst

Heterogeneous catalysts are utilized in OSR. There are three major considerations in selecting catalyst material for OSR, which are [17]:

1. Catalyst is required to be active and selective for both SR and POX major/desired reactions
2. Catalyst should be thermally stable at high operating temperature of OSR (up to 800^{o}C). At high temperature, sintering/agglomeration of catalytic metal are the major threat.
3. Catalyst should be chemically robust due to complex reactions involved. Catalyst must maintain structural integrity in both oxidizing and reducing condition, and it also must be resistant to carbon formation and sulphur poisoning.

Various catalysts for OSR process have been investigated and reported with respectful advantages and disadvantages for each. Ranging from noble metals to cheaper base metals, a wide selection of catalysts for OSR is available in the market as commercial ones, while novel catalysts are mostly in-house produced with limited or specific uses. Investigated OSR catalysts are mostly the same as applied in SR. It was reported by Jones et al. [23] that the activity order of most used catalysts for methane SR is Rh, Ru > Ni > Pt > Pd > Co. However, further research on pyrolysis oil aqueous phase reforming, which is represented by aqueous ethylene glycol reforming, indicated that silica supported Pt or Ni based catalysts show better activity compared to Ru, Rh and Pd [31].

Two different materials are used as catalysts and support in this study, which are nickel and zirconia. Nickel will be the main catalyst to be investigated. Zirconia will be used both as a separate catalyst on monolith and in form of in-house zirconia supported nickel catalyst. Both materials will be discussed below.

3.2.1 Nickel

The most investigated catalyst for OSR is nickel based catalysts, which offer favourable commercial aspects such as appreciable activity, competitive price and abundant availability [17]. Despite the advantages, drawbacks of Ni-based catalysts are high sintering rates and carbon formation compared to noble metal catalysts. Ni sintering temperature starts from 590^{o}C [24], which are lower than usual OSR operating temperature. Thus, to overcome the limitation of faster deactivation, Ni catalyst is mostly prepared with higher loadings to obtain sufficient activity and reach the chemical equilibrium. Another concern regarding Ni-based catalysts is the tendency to be oxidized by gas phase oxygen [17]. Oxidized nickel promotes the combustion of carbon compounds, thus leading to decrease in H_2 and CO yields and triggering creation of hot spots and high temperature gradient along the catalyst bed [17].

Nickel catalyst are usually supported on alumina (Al_2O_3) which has high surface area, good pore distribution and size, acid/base sites and good thermal stability. The most common alumina used to support nickel is γ-Alumina that can stand temperature up to 1,200^{o}C. However, the acidic sites on alumina tend to promote acceleration of coke formation. Thus alkali dopants are usually added or basic support such as MgO, CeO_2 and ZnO is used to reduce the acidity sites tendencies [31]. Some other supports for nickel catalyst that have been investigated for bio-oil steam reforming are ZrO_2 and CeO_2–or combination of these supports [31, 41].

3.2.2 Zirconia

Zirconia is known to be a new more inert catalyst support compared to more traditional supports such as silica or alumina [37]. However, zirconia is also used for other purposes, such as active part of catalyst and as a promoter. For example, zirconia is used as catalyst in gas cleaning system. Zirconia is known for its ability to perform as a selective catalyst for tar and ammonia oxidation with high conversion even at mild temperatures below 600^{o}C. Furthermore, alumina-doped zirconia is also resistant to poisoning by H_2S, which is a typical catalyst poison in gasification and reforming process [38].

The most stable phase of zirconia is discovered to be the monoclinic phase, which can withstand temperatures of up to 1170^{o}C although with significant surface loss when calcination temperature is increased from 450^{o}C to 900^{o}C [37]. The stability can be increased by the addition of species such as Ce, Y or La.

3.2.3 Catalyst Deactivation

There are several catalyst deactivation mechanisms that can occur during the OSR process. Most of them are closely related to steam reforming process under specific catalyst type. As nickel is one of the most common catalysts being used for OSR, this section will mostly discuss about the deactivation phenomena in nickel-catalysed steam reforming system. Note that these deactivation

mechanisms might also be valid for other catalysts and each of them has different rate of deactivation.

In general, there are three different main deactivation mechanisms of Ni-based catalysts during SR, which are thermally induced deactivation, carbon formation and sulphur poisoning [25]. All of them significantly affect the catalyst activity.

3.2.3.1 Thermally Induced Deactivation

Reforming, including OSR, is often carried out at elevated temperature around 700-900^{o}C, which pushes the thermal stability of the catalyst material to the limit. Typical causes of thermal deactivation of reforming catalyst are [26]:

- Structural transformation of support material: (e.g. collapse of pore structures)
- Sintering of supported metal cluster: thermally induced coalescence of crystallite/active metal clusters
- Solid-solid interaction: between active part and its support which creates inactive compounds

In heterogeneous catalyst, the active metal/crystallite is usually spread over a support material as small particles. In some cases, the metal particles can agglomerate, which is commonly known as sintering process. The process is temperature and pressure dependant and occurs above different temperature limits for different materials. There are two mechanisms for the metal particle growth being proposed [25], which are:

- Particle migration, where the entire crystallites migrate over the support, followed by coalescence.
- Ostwald ripening, which is known also as atom migration or vapour transport, where metal transport species emitted from one crystallite, migrate over the support or carried by the flow phase and captured by other crystallites.

Despite the mechanism, sintering results in activity problem due to loss of active surface area and uneven distribution of the active substance on the support. The structural transformation can also result in catalyst loss in certain type of reactors, in which high gas velocity might push crumbled catalyst particle out of the bed.

3.2.3.2 Carbon Formation

In fuel processing and hydrocarbon involved reactions, deposition of carbon containing species on metal catalyst is inevitable [26, 27]. There are three types of carbon that have been observed in a reformer [25]:

1. *Pyrolytic carbon*: resulted by exposure of long-chained hydrocarbons to high temperature. Usually triggered by hot bands in the catalyst bed due to sintering and sulphur poisoning phenomena.
2. *Encapsulating carbon (gum)*: formed during reforming of heavy hydrocarbons containing aromatic compounds. Deactivation due to gum carbon usually indicated by drift of the temperature profile in the catalyst bed without increase in the pressure drop.
3. *Whisker carbon*: Known as the most destructive carbon deposit on nickel catalysts, whisker carbon is formed mostly due to low S/C ratio.

Pyrolytic carbon occurs at high temperature (>600^{o}C) through gas-phase reactions which form unsaturated molecules and radicals that undergo dehydrogenation and polymerization. Encapsulating carbon occurs at temperatures around 500^{o}C, and it consists of a thin CH_x film or few graphite layers covering the nickel. Encapsulating carbon's effect is similar to sulphur poisoning. Whisker carbon is a filament like carbon formed due to hydrocarbon or CO dissociation on one side of nickel particle and nucleation of graphite carbon as the whisker on the other side [25].

Carbon formation in the reforming reactor may be the cause of several harmful effects such as [25]: increased pressure drop, crushed catalyst pellets, blockage of the active metal surface or carbon formation at the inner perimeter of the reactor tubes resulting in a lower heat transfer coefficient. Thus, it is important to limit carbon formation in the reforming process.

Carbon deposition is related to the proportion of oxidizing agent in the feed gas and temperature. Increasing O/C and S/C ratio, as well as increasing the reactor temperature will significantly reduce the amount of carbon deposition [26]. Note also that the deactivation caused by carbon deposition is generally reversible. Coke can be partially removed by introducing oxidant agent into the deactivated catalyst, where carbon will be transformed into carbon monoxide or carbon dioxide.

3.2.3.3 Sulphur Poisoning

Most virgin or fresh biomass contains little to no sulphur, while biomass derived feedstock (i.e. municipal solid waste, sewage sludge) does contain sulphur [28, 29]. The sulphur content of biomass is usually lower than 0.5%-wt (db) [29] with variations coming from different type of feedstock. Woody biomass contains less sulphur than herbaceous biomass and biomass derived fuels.

Sulphur is a severe poison in the reforming catalyst, especially for nickel catalyst. It has been investigated that the deactivation by sulphur poisoning is high for nickel catalyst below 700^{o}C [25, 26]. At the reforming conditions, sulphur in the feed will be converted mostly into H_2S, hydrogen sulphide. H_2S will then be adsorbed strongly on metal surface, limiting the ability of the metal to adsorb other compounds [9], as shown in Eq. (23) [26].

$$H_2S + Me^0 \rightarrow MeS + H_2 \tag{23}$$

Although many feedstock desulfurization pre-treatment technologies are available, sulphur containing compound in the feed might still reach the catalyst

at a ppb level and still be dangerous [25]. It is also observed that the effects of sulphur on the reforming catalyst tend to be cumulative, so that even low levels of sulphur can eventually deactivate the catalyst [26]. The effect of sulphur poisoning includes decrease in catalyst activity, followed by increase of wall temperature of the reactor due to lower heat absorption by the endothermic reactions. It is noticed that higher coking might also be resulted due to higher chance for longer-chained hydrocarbons not to be converted due to catalyst active site loss. However, it is investigated that sulphur poisoning inhibits coke formation, especially whisker type, on the catalyst surface [25, 30].

3.3 System Design

3.3.1 Reactor Type

Most of experimental and the model systems studies for steam reforming have been carried out in a fixed-bed reactor. Despite the convenience it provides, reaction performance in fixed-bed reactor may suffer for instance from uneven temperature distribution in the reactor and low heat transfer efficiency [31]. Meanwhile, industrial scale reactor for methane reforming also adopts this fixed-bed concept, by using a set of tubes filled with catalyst, which are heated by radiation in various types of tubular furnace [32]. However, due to different characteristics of feedstock, reforming of pyrolysis-oil and its derived feedstock face different challenges.

Czernik et al. [33] suggested that steam reforming for pyrolysis oil could be economically competitive with conventional H_2 produced from methane reforming in terms of production cost. The idea was to develop a regionalized system of H_2 production with small and medium-sized pyrolysis oil plants (<500 Mg/day) providing pyrolysis oil as the feedstock for hydrogen production. Using similar operating condition as in commercial steam reforming processes, 80% H_2 yield from theoretical amount was obtained from pyrolysis oil [34]. However, high formation rate of carbonaceous deposits was observed, especially in the

upper layer of the catalyst bed and the reactor freeboard, which limited the operation to short period of time. Thus, Czernik et al. developed a fluidized bed reactor for the steam reforming of pyrolysis-oil.

Fluidized bed is proven to provide better catalyst stability compared to fixed-bed reactor due to a better contact between catalyst and the oxidizing agent. The H_2 yield remained stable around 77% from its maximum stoichiometric limit and could be increased up to 95% with additional steam [40] during the designated time. The research also suggests fluidized bed reactor as a promising solution to improve H_2 production from complex hydrocarbon feedstock. Other suggestion comes from Kechagiopoulos et al.[35] with novel spouted-bed reactor, which was proved to supress the coking rate from pyrolysis oil derivatives reforming. Table 5 shows the advantages and disadvantages of each reactor type to be used for oxygenated hydrocarbon feedstock reforming.

TABLE 5Advantages and disadvantages of several option of catalytic steam reforming reactors

	Fixed-bed	**Fluidized-bed**	**Spouted-bed**
Advantages	Simple operation, easy to model, suitable for commercial catalyst	Good catalyst stability, reduce in coking, high operating time.	Reduce in coking, high operating time.
Disadvantages	High carbonaceous compound formation rate, limited operating time, catalyst regeneration is needed frequently.	Strong catalyst material (especially support) is required due to catalyst attritions.	Strong catalyst material (especially support) is required due to catalyst attritions.

3.3.2 Feeding System

Although many attempts on steam reforming of pyrolysis oil and its aqueous fraction had been showing positive results, there is one challenge that is mentioned in many publications. This problem is related to the feeding system of the feedstock into the reactor. Compared to conventional fossil fuel, biomass-based feedstock has low hydrogen to carbon ratio, which indicates a high coke formation potential [31]. Biomass derived feedstock also has stability issue and

decomposes easily under the reforming conditions. It was found that several main components in biomass feedstock has different rate of coke formation during the gasification or reforming process; it was found to decrease in following order: glucose >> m-xylene > acetone > ethylene glycol > acetic acid [20].

Czernik et al. [34] mentioned that accumulation of carbonaceous compounds was found between the nozzle and the catalyst bed in a fixed-bed reactor, indicating the ease of coke formation in early stage of the reactor. This phenomenon can be explained as sugar compounds are mainly found in the aqueous fraction of pyrolysis oil and are difficult to vaporize. As a consequence, the risk of carbon formation that can clog the feeding system is high. Thus, the feeding system should be well designed to avoid any coke formation that can clog the whole feeding systems.

4. State of The Art

State of the art of hydrogen production from bio-oil is presented in Table 6, covering several recent and important findings on the related area of hydrogen production via pyrolysis oil and its aqueous fraction. Many of the references taken were productive in this area; Wang, Czernik and Chornet were the front runners in introducing catalytic steam reforming process of pyrolysis oil and its aqueous fraction. This thesis itself will be among the firsts to use real aqueous fraction for oxidative steam reforming.

4.1 Challenges in Hydrogen Production from Pyrolysis Oil

Hydrogen has been a very important substance for producing basic chemical products as well as being noticed as future energy carrier. Based on the previous section, many attempts have been done to utilize pyrolysis oil in hydrogen production as an option of upgrading. The most common approach is feeding pyrolysis oil (and its derived product such as pyrolysis oil aqueous-phase) into well-known catalytic processes such as steam reforming, partial oxidation, or autothermal reforming, which have been commercially used for fossil fuel based feedstock. Most of them also adapted same catalysts and process conditions from commercial hydrogen production from fossil fuels.

TABLE 6 State of the art of hydrogen production from pyrolysis oil

Hydrogen Production from Pyrolysis oil	Model compounds	Thermodynamic analysis	Aqueous phase steam reforming	Aqueous phase methanol, acetic acid and ethylene glycol, 340-660K, P_{sys}/P_{H2O}=0.1-2.0, influence of CaO and O_2	Xie et al. (2011)
		Experimental	Catalytic steam reforming	Phenol, acetic acid and hydroxyaceton (individual test), Ni/nano-Al_2O_3 and Ni/ɣ-Al_2O_3 catalysts, 500-800^oC	Wang et al. (2014)
				Ethylene glycol (aq. phase model), Ni/Olivine catalyst, 650-800^oC, spouted-bed reactor, S/C=4.6	Kechagiopoulos et al. (2007)

TABLE 6 State of the art of hydrogen production from pyrolysis oil (cont.)

Hydrogen Production from Pyrolysis oil	Whole/Oil fraction	Thermodynamic Analysis	Autothermal Steam Reforming	Combined nickel monolith and PGM monolith catalyst, pilot scale	Leijenhorst, (2013)
		Experimental	Partial Oxidation (POX)	Bio-oil with methanol addition 10-50%, a-Alumina foam monoliths catalyst, C/O 0.4-0.9, 550-1000^{o}C	Rennard et al., (2010)
				Novel Y-type reactor, NiO/ Al_2O_3 (30 %-wt) catalyst, 550-800^{o}C, atm pressure.	Hu & Lu (2010)
			Steam Reforming	Novel Y-type reactor, NiO/ Al_2O_3 (30 %-wt) catalyst, 550-800^{o}C, atm pressure.	Hu & Lu (2010)
			Staged POX & SR	Bio-oil with methanol addition 10-50%, a-Alumina foam monoliths catalyst, C/O 0.4-0.9, 550-1000^{o}C	Rennard et al. (2010)
			Autothermal/ Oxidative Steam Reforming	Novel Y-type reactor, NiO/ Al_2O_3 (30 %-wt) catalyst, 550-800^{o}C, atm pressure.	Hu & Lu (2010)
				Packed bed, 0.5% Pt/Al_2O_3 BASF catalyst, 800-850^{o}C, GHSV= 2000 h^{-1}, S/C=2.8-4.0, O/C=0.9-1.1	Czernik & French (2014)
	Aqueous fraction	Experimental	Catalytic steam reforming	Fixed bed, commercial Z417 catalyst + CaO/dolomite bed as sorbent (carbon capture concept), 500-700^{o}C	Yan et al. (2010)
				Fluidized bed, NiO/MgO catalyst, 550-850^{o}C, WSHV 0.6-1.4 h^{-1}, S/C=4-10	Zhang et al. (2011)
				Fluidized bed, Ni-Al catalyst modified with Ca & Mg, 650^{o}C, GSHV 12000 & 5400 h^{-1}	Medrano et al. (2011)
				Fluidized bed, phase separation, commercial nickel catalyst, 800-850^{o}C, atmospheric, S/C=7-9, GHSV 700-1000 h^{-1}	Czernik et al (2012)
				Fixed bed, Ni-based and ZrO_2 catalyst, 600-750^{o}C, 30-120 min residence time, atm pressure	Sánchez (2013)
				Fixed bed, Ni/Al co-precipitated catalyst with varying nickel content (22-33%), 600-800^{o}C, S/C=5.58	Bimbela et al. (2013)
				Fixed bed, Modified sepiolite catalyst with Ni or Mo, 700-800^{o}C, S/C=16-18	Liu et al. (2013)

Although positive results have been obtained on hydrogen production from pyrolysis oil, the technology is far from mature. There are challenges faced and discussed by several researchers. These challenges are summarized in three main points:

1. *Feedstock Complexity*

   Pyrolysis oil and its derivatives are complex feedstock for steam reforming, since they contain mostly oxygenated hydrocarbons with distinct chemical and physical properties which have profound impacts on the reforming process. The feedstock is mainly characterized with low hydrogen to carbon ratio compared to conventional fossil fuels, indicating a high risk of coke formation during the gasification process. Many oxygenated compounds also have low thermal stability which leads to decomposition or polymerization of the compounds before they reach or go through the catalyst bed.

   As pyrolysis oil has high degree of functionality, this feedstock tends to be highly reactive. As a consequence, the selectivity of product is low due to many reactions might occur and generate a broad range of products. It is often necessary to have multiple conversion steps to increase the yield of the desired product. Apparently, this problem also leads to economic issue.

2. *Reactor Design*

   Most of today's reforming plants are using natural gas as their feedstock. Feeding a liquid hydrocarbon into reforming reactor affects the reactor design. Different types of reactors have been used in the studies: from fixed bed to novel reactor design. However, most of the researches faced the same problem, which is the feeding system.

   Sprayer is mostly used as a solution to feed pyrolysis oil into the catalyst. This method allows the feed to be distributed more evenly and increase the

surface area. However, as discussed in the first point, oxygenated compounds also have low thermal stability, which tends to promote coke formation. This problem is also faced even when sprayer is used. Sugars are mainly hard to vaporize thus creating problems in the feeding system such as clogging. Thus, a special attention should be given to the feeding system prior to successful feeding process.

Reactor configuration is another challenge faced by hydrogen production from bio oil via reforming. Fixed bed has limitations in avoiding coke formation, especially on the wall between feeding system and the catalyst bed where polymerization usually occurs. On the other hand, fluidized bed—which is harder to be modelled—has typically catalyst attrition problems. Although several novel reactors had been proposed, this problem remains as big challenges in finding the right reactor configuration designed specifically for pyrolysis oil and its derivatives reforming process.

3. Catalyst Lifetime

Many of pyrolysis oil reforming attempts were carried out using commercially available catalyst for fossil fuel reforming, such as Ni-based catalyst. Despite its good activity and decent selectivity, pyrolysis oil reforming tends to deactivate the catalyst faster than fossil feedstock. Several ways had been reported to decrease the deactivation rate which is mainly caused by carbon deposit on catalyst surface, such as addition of excess steam and oxygen. This issue creates a barrier of process efficiency because continuous regeneration of catalyst is needed. Thus, finding reliable catalysts or optimum ways to avoid catalyst deactivation are listed as challenges in this area.

5. Experimental Part

Steam reforming of pyrolysis oil aqueous fraction has been conducted by several researchers with positive results and being further investigated by many, as the system still have lots of challenges to overcome. The experimental part of this thesis aims to investigate the effect of oxygen concentration to the conversion of pyrolysis-oil aqueous fraction into hydrogen with three different catalysts, which are a commercial nickel catalyst, a combination of zirconia monolith and commercial nickel catalyst, and an in-house made nickel over zirconia monoclinic catalyst by VTT, Technical Research Centre of Finland. The oxygen variations will be represented in O/C ratios. The tests will be carried out in steady process conditions, which is temperature of 650^{o}C in atmospheric pressure. The aimed outcome is better and more stable catalyst activities, increased hydrogen production rate and carbon conversion due higher O/C ratio, as predicted by the theory behind oxidative steam reforming.

5.1 Material and research method

5.1.1 Feedstock

The feedstock of the system is pyrolysis-oil aqueous fraction from a pilot scale fast pyrolysis plant at VTT, Technical Research Centre of Finland. The pyrolysis plant used forest residues (pine, spruce and birch wood) as the feed. The composition of the aqueous fraction had been analysed by VTT and it is shown in Table 7. In summary, there is 27.3 wt-% of organics in the feed and the rest is water. This value corresponds to S/C ratio of 3.84 and O/C ratio of 0.67.

Two main assumptions were made to simplify the aqueous fraction composition. The first assumption was to represent sugar-type compounds as levoglucosan, which is most abundant sugar compound in common pyrolysis oil aqueous fraction [14, 44, 45]. Second assumption was that all the unidentified compounds

were described by a molecule with chemical formula of $C_8H_{10}O_3$. This formula was decided based the longest retention time of the unidentified compounds in the gas chromatograph that are heavier than 4-Ethylcatechol, which has a similar formula.

TABLE 7 Composition of pyrolysis oil aqueous fraction from VTT's fast pyrolysis Process Development Unit via fractional condensation of pyrolysis vapours

Compound	wt-%	Compound	wt-%
Acetaldehyde	0.269	Caproic acid	0.010
Furan	0.039	Guaiacol/Vanillic acid	0.051
Acetone	0.110	4-Methylguaiacol	0.029
Methanol	1.978	o-Cresol	0.005
2-Butanone	0.037	Phenol	0.017
Isopropanol	0.015	4-Ethylguaiacol	0.004
Ethanol	0.003	m-cresol	0.008
2-Pentanone	0.010	2-Propylphenol	0.003
n-Propanol	0.005	Eugenol	0.004
1-Hydroxy-2-Propanone	2.655	4-Ethylphenol	0.005
Glycolaldehyde	0.779	o-Vanillin	0.021
1-Hydroxy-2-Butanone	0.077	Syringol/4-Propylphenol	0.010
Acetic acid	11.57	Isoeugenol	0.023
Furfural	0.338	5-(Hydroxymethyl)-furfural	0.043
2-Acetylfuran	0.018	4-Methylcatechol	0.003
Propanic acid	0.015	4-Ethylcatechol	0.022
Isobutyric acid	0.018	Sugars (Assumed as Levoglucosan)	4.300
5-Methylfurfural	0.023	Unknown (Assumed as C8 compound)	4.700
Butyric acid	0.063	**Total Organic**	**27.30**
Valeric acid	0.026	**Water**	**72.70**

The aqueous fraction for this experiment was collected directly from hot condenser unit of VTT's fast pyrolysis Process Development Unit via fractional condensation of the pyrolysis vapours. The vapours were quenched in the scrubbers at a temperature of 65°C. The aqueous fraction, which consists mostly of water and light molecular weight organics, was collected from a secondary condensation system. This technique results in a higher content of organic compounds compared to aqueous fraction produced via water solvent extraction during phase separation process [14], which usually results in aqueous fraction with water content between 77-84% [35, 40, 43].

The composition of pyrolysis oil aqueous fraction depends on pyrolysis feed type and quality, pyrolysis operating conditions and condensation sequence. In this study, the empirical formula of the dry aqueous fraction was defined as $CH_{1.44}O_{0.67}$ which was calculated based on the chemical formula and molar fraction of each detected and assumed compound. This dry organic value corresponds closely to other formulas reported in different literatures, i.e. $CH_{1.25}O_{0.55}$ [46] and $CH_{2.39}O_{0.71}$ [43].

5.1.2 Catalyst

Three catalysts were used during the experiment; one of them is commercial catalyst and two in-house made catalysts. The catalysts were (1) commercial nickel catalyst (Reformax) with pellet size of 3x3 mm, (2) patented [47] washcoated zirconia on ceramic monolith (WO 2012/022988, WO 2007/116121) doped with cerium and lanthanum and (3) VTT in house made Ni/ZrO_2, which is nickel impregnated on monoclinic zirconia (Saint-Gobain NorPro) . Due to different density of commercial nickel and in-house Ni/ZrO_2, inert material (silicon carbide (SiC), 1.25 mm) was used with the in-house made catalyst to achieve around the same WHSV (weight hourly space velocity) and GHSV (gas hourly space velocity). Zirconia monolith was only used as pre-reformer catalyst, not a stand-alone catalytic system.

5.1.3 Reactor System

The experiment of steam reforming of pyrolysis oil aqueous fraction was conducted in an atmospheric Ø2.66cm x 50cm fixed bed steel reactor. The system was used previously by Sánchez but several adjustments were done after his thesis, e.g. pump type was changed and the feeding system was improved, as suggested by the same thesis report [42]. The feeding system consists of two nozzles, one of which carries the aqueous fraction and the other one blows a mixture of nitrogen and air flow at 1.9 L/min (NTP). The flow was chosen in order to create a good and even spraying of aqueous fraction feed onto the catalyst

bed. An isocratic pump was used for this experiment, replacing a HPLC (high pressure liquid chromatograph) pump used in Sánchez [42]. A simplified diagram of the system is shown in Figure 6.

The reactor was placed inside a three zone furnace. A thermocouple pocket with a diameter of 0.4 cm was also included in this reactor, which was fixed to monitor the catalyst bed temperature profile from top to bottom. The produced gas flowed through a condenser to separate the water and passed through gas washing bottles (containing iso-propanol and water in ice bath) before analysed. The analysis of product gas included real-time gas analysis by ABB gas analyser model AO2020 for H_2, CO, CO_2 and CH_4, and also gas chromatograph by HP model 5890 Series II to analyse compounds present in small quantities, mainly C_2 compounds (including C_2H_2, C_2H_4 and C_2H_6).

The experiments were carried out at VTT Research Centre of Finland. Each experiment had three steps: reduction, main experiment and coke burning. In the reduction process, nickel oxide in the catalysts was reduced at 850^{o}C for 1 hour with a 1.1 L/min gas containing 50 % H_2 and 50 vol-% N_2 to be activated. After reduction, the temperature was adjusted near the reaction temperature. The main experiment was then conducted with gas composition adjusted with each O/C ratio variation. The total gas flow remained the same for the whole variations, which was 1.9 L/min and the feed flow was 0.4 mL/min. During the main experiment, the temperature at top of catalyst bed was monitored, while oven temperature was adjusted to achieve temperature of around 650^{o}C. This temperature was chosen based on conclusion of Sánchez [42], where it was found that 650^{o}C is the most optimum temperature due to chemical equilibrium of steam reforming and water shift gas reaction. At this temperature, steam reforming is favoured over water shift gas reaction, resulting in the highest possible outcome of hydrogen in the output stream [51, 52, 53]. This main experiment lasted for 4 hours.

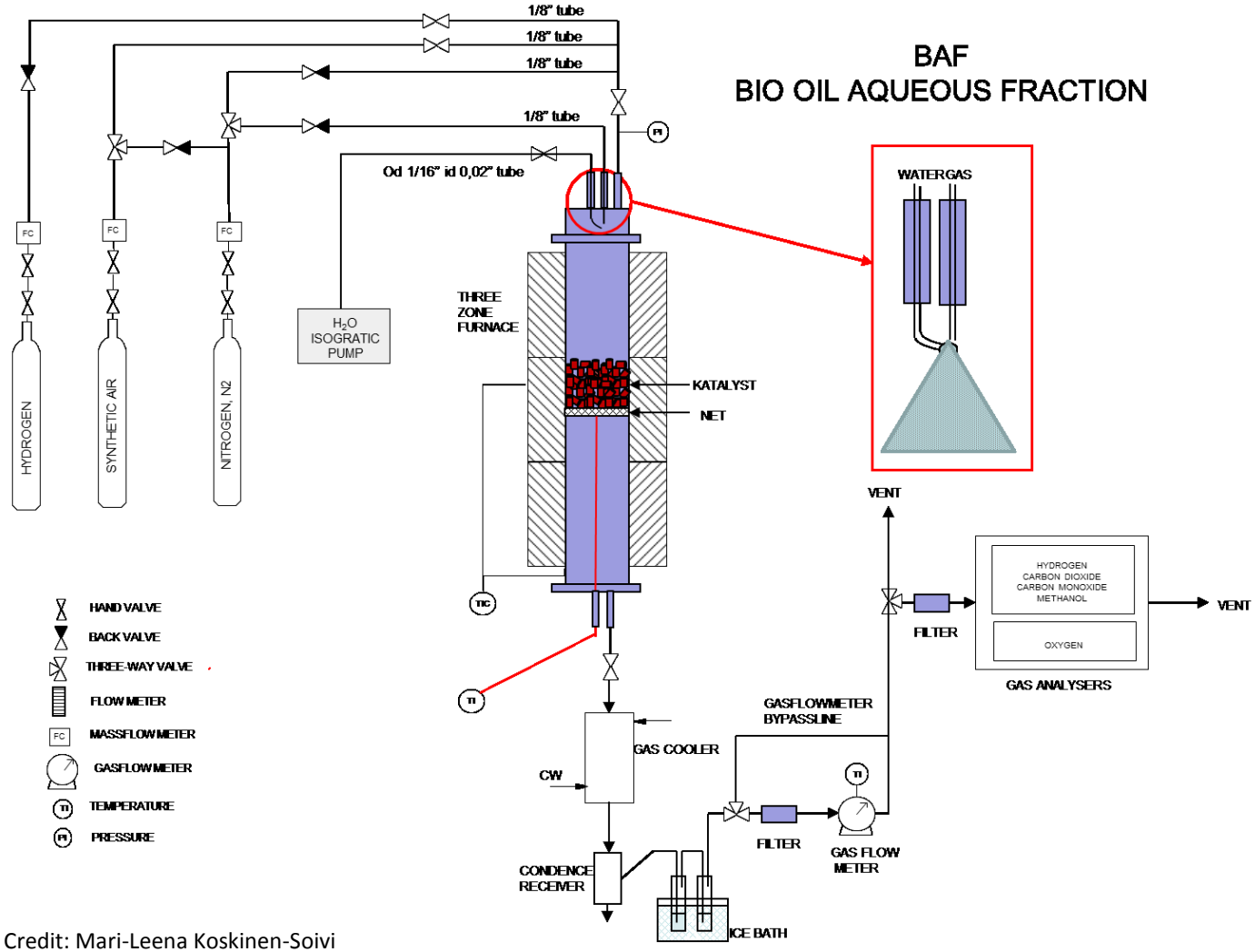

Credit: Mari-Leena Koskinen-Soivi

FIGURE 6 Simplified diagram of reactor system for steam reforming of pyrolysis oil aqueous fraction

After the main experiment, the reactor was purged by N_2 and oven temperature was raised to 850^{o}C. Oxidation of catalyst cokes and carbon deposits was carried out after by feeding the system with 1.5 L/min of mixed gas containing 38 vol-% air and 62 vol-% N_2 for 1 hour. The remaining carbon deposit and wall cokes were weighed after the burning had ended.

6. Results

6.1 Carbon to Gas Conversion and carbon balance

Carbon to Gas (C2G) conversion shows how much feed was converted into product gases. In these experiments four gases were monitored real time to determine the conversion. The monitored four gases were CO_2, CO and CH_4. Table 8 shows the overall result of C2G conversion for each variation.

TABLE 8 Carbon-to-gas conversion for each experiment variation

Catalyst	Run	Run Hour	O/C Ratio	C2G Conversion (%)
NiO Reformax	BAFA-4 (base)	4	0.67	86
	BAFA-14	4	0.88	82
	BAFA-7	4	0.95	74
	BAFA-6	4	1.10	81
ZrO_2 Monolith + NiO Reformax	BAFA-10 (base)	4	0.67	85
	BAFA-12	4	0.88	81
	BAFA-13	4	0.95	86
	BAFA-18	4	1.10	86
VTT's Ni/ZrO_2	BAFA-9 (base)	4	0.67	83
	BAFA-17	4	0.88	77
	BAFA-15	4	0.95	86
	BAFA-16	4	1.10	67

It can be seen from Table 8 that C2G conversion has no solid correlation either to O/C ratio or to catalyst type used. The number varies between 67-86% and lowest conversion was observed with different O/C ratio for different type of catalyst used. To investigate this phenomenon more closely, hourly C2G conversion was plotted to see if there is any change of C2G conversion between time to time in the system. Figure 7 shows the hourly C2G conversion for each catalyst with different O/C ratio.

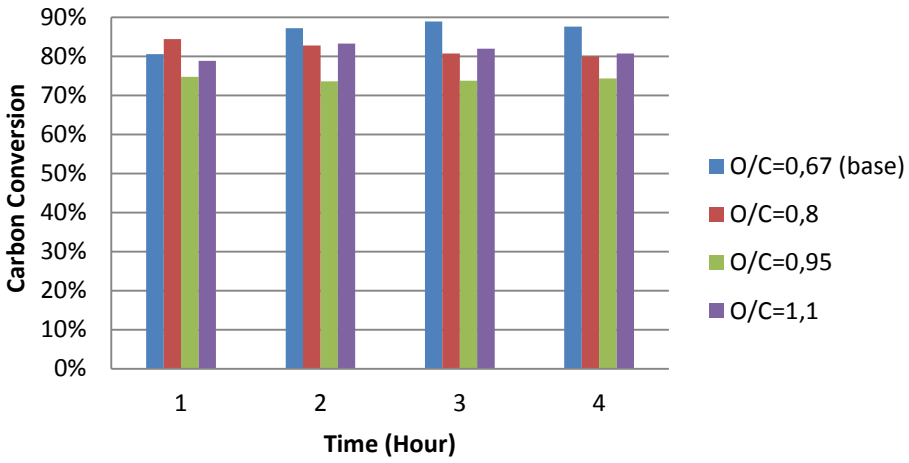

(a)

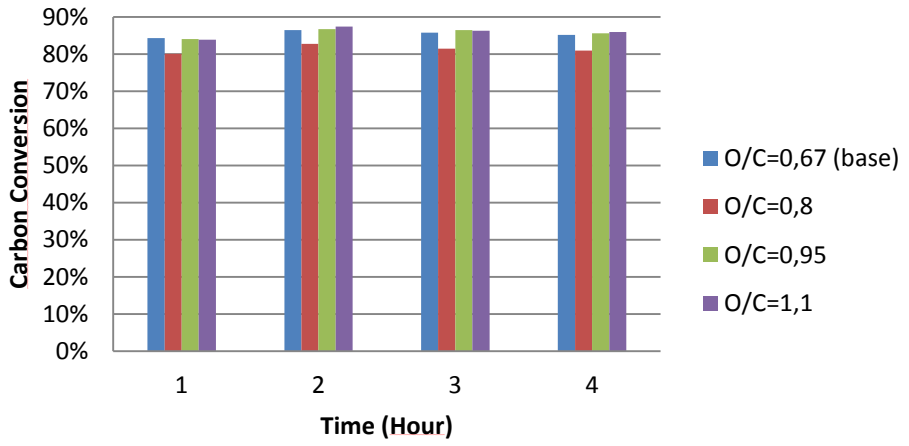

(b)

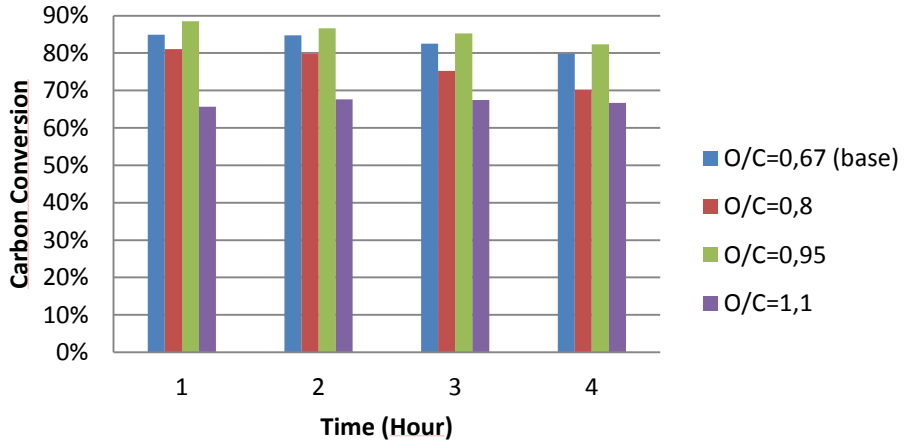

(c)

FIGURE 7 Hourly (average) carbon-to-gas conversion during pyrolysis oil aqueous fraction steam reforming at 650oC using (a) Reformax, (b) Zirconia Monolith + Reformax and (c) VTT's Ni/ZrO2 catalyst in different O/C ratios.

From Figure 7, it can be seen that with different O/C ratios, the stability towards the carbon conversion values were changing although the tendencies did not apply for all type of catalyst.

TABLE 9 Total carbon balance for each variation experiment

Catalyst	Run	Run Hour	O/C	Total Carbon Balance (%)
NiO Reformax	BAFA-4 (base)	4	0.67	94.8
	BAFA-14	4	0.88	95.0
	BAFA-7	4	0.95	84.5
	BAFA-6	4	1.10	93.2
ZrO2 Monolith + NiO Reformax	BAFA-10 (base)	4	0.67	97.0
	BAFA-12	4	0.88	93.2
	BAFA-13	4	0.95	95.1
	BAFA-18	4	1.10	94.5
VTT's Ni/ZrO2	BAFA-9 (base)	4	0.67	94.1
	BAFA-17	4	0.88	88.7
	BAFA-15	4	0.95	96.1
	BAFA-16	4	1.10	76.7

For Reformax catalyst (Fig. 7a) and VTT Ni/ZrO_2 (Fig. 7c), it was observed that higher O/C ratio tends to stabilize the C2G conversion within the 4 hours' time-on-stream. The blue bar in Fig. 7a, which indicates the lowest O/C ratio, shows a fluctuating conversion values. Meanwhile, higher O/C ratios which were indicated by other bar colours show a better stability over time; steadier bar heights with less fluctuating profiles. Same tendencies were appeared for VTT catalyst where the purple bars in Fig. 7c, which indicates the highest O/C ratio, shows the steadiest conversion among the other lower O/C ratios. However, additional oxygen to the catalyst combination system gave no further effect. It can be seen that the conversion values for the whole variation of O/C of zirconia monolith + Reformax catalysts remained constant throughout the experiments.

During the burning of the catalyst, carbon deposit on the catalyst was converted into CO and CO_2 which was also monitored for 1 hour. The catalyst for every batch was also weighted before reaction and after carbon burning to see if there was any carbon deposit on its surface.

Table 9 shows the carbon balance for each batch of experiment. The total carbon balance is a summation of C2G conversion, wall coke and amount of CO and CO_2 gases monitored during the burning of carbon deposit step (catalyst burned deposits).

Almost all the experiments showed carbon balance above 90%, except BAFA-7, BAFA-17 and BAFA-16. Apart from these three exceptions, the carbon closure for each experiment was satisfactory. However, combination of zirconia monolith + Reformax showed the best consistency and the highest overall of total carbon balance.

6.2 Hydrogen Yield

The main product of pyrolysis oil steam reforming is hydrogen which was monitored real time using gas analyser. Hydrogen yield represents the amount of hydrogen produced compared to the amount of hydrogen that can be produced stoichiometrically. Table 10 shows the hydrogen yield for each experiment. Note that for higher O/C ratio, the maximum hydrogen yield that can be produced is getting lower.

From Table 10, it can be seen that without any addition of oxygen, Reformax catalyst gave the highest overall hydrogen yield, followed by a slightly lower yield with zirconia monolith + reformax system and significantly lower yield when VTT's Ni/ZrO_2 was used. From the same table, a visible tendency of decrease of overall hydrogen yield can be observed when O/C ratio is increased regardless the catalyst used regardless type of catalyst used. In this sense, combination of

zirconia monolith + Reformax exhibits the mildest decrease of yield with increasing O/C ratio.

The hydrogen production is commonly presented in term of amount of hydrogen produced over amount of feed being fed into the system. Figure 8 shows the mass yield of hydrogen production in this sense. It can be seen that addition of oxygen is indeed correlated negatively to hydrogen production regardless type of catalyst used.

TABLE 10 Hydrogen yield and hydrogen production result from steam reforming of pyrolysis oil aqueous fraction using different catalysts and O/C ratios

Catalyst	Run	Run Hour	O/C	H2 Yield (%)	H2 Production (g/100g feed)
NiO Reformax	BAFA-4 (base)	4	0.67	81	3.47
	BAFA-14	4	0.88	77	2.98
	BAFA-7	4	0.95	68	2.54
	BAFA-6	4	1.10	72	2.44
ZrO2 Monolith + NiO Reformax	BAFA-10 (base)	4	0.67	79	3.42
	BAFA-12	4	0.88	78	3.02
	BAFA-13	4	0.95	76	2.82
	BAFA-18	4	1.10	74	2.53
VTT's Ni/ZrO2	BAFA-9 (base)	4	0.67	73	3.16
	BAFA-17	4	0.88	68	2.63
	BAFA-15	4	0.95	69	2.56
	BAFA-16	4	1.10	65	2.20

Just like the investigation for C2G conversion, hydrogen yield was also calculated as a function of time-on-stream to see the production stability during the experiment. Figure 9 shows the hourly hydrogen yield for each experiment.

When Reformax was used with only small oxygen addition (Fig. 9a, red bar) it can be clearly seen that the hydrogen yield was decreasing over time (around 9% decreases). When the O/C ratio was increased, the yield was getting stable overtime. Meanwhile, addition of pre-reformer zirconia monolith catalyst (Fig.

9b) increased the stability of Reformax pictured by stable blue bars over time, which means even without oxygen addition the yield became stable (decrease ≤4%).

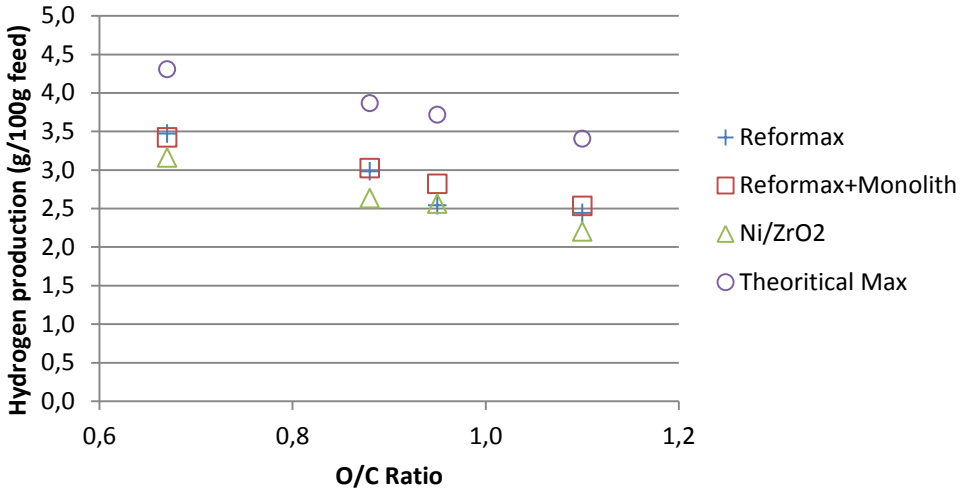

FIGURE 8 Hydrogen production of oxidative steam reforming of pyrolysis oil aqueous fraction with different catalysts and O/C ratios compared to maximum theoretical hydrogen production

Addition of oxygen in the zirconia monolith + reformax system shows very good stability with ≤3% differences of hydrogen yield over 4 hours of time-on-stream for all variations of O/C ratios. Furthermore, zirconia monolith addition also resulted in more gradual decrease of hydrogen yield with increase of O/C ratio. On the other hand, VTT's Ni/ZrO2 catalyst (Fig. 9c) shows poor stability over time, indicated by significant decreases of hydrogen production. However, a quite stable yield was achieved with O/C ratio of 1.10 (Fig. 9c, purple bar) where the yield change was ≤5%.

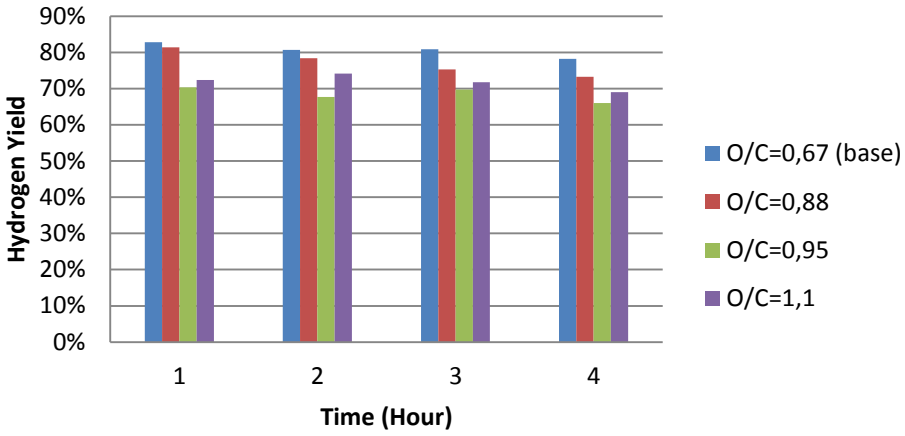

(a)

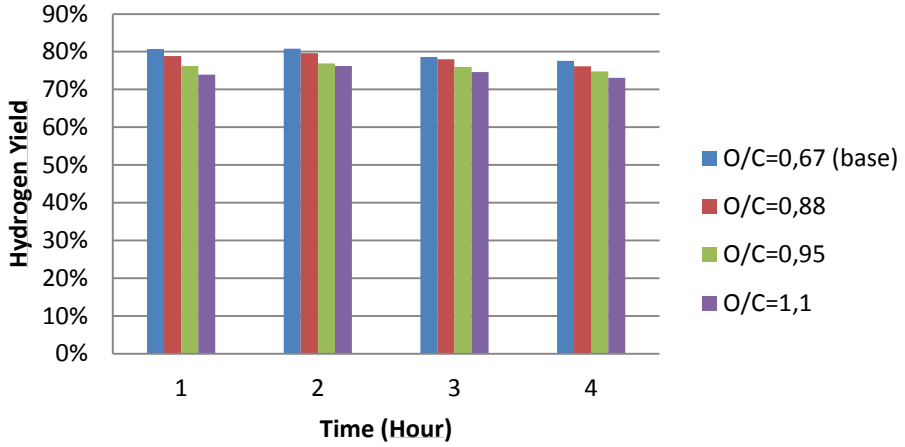

(b)

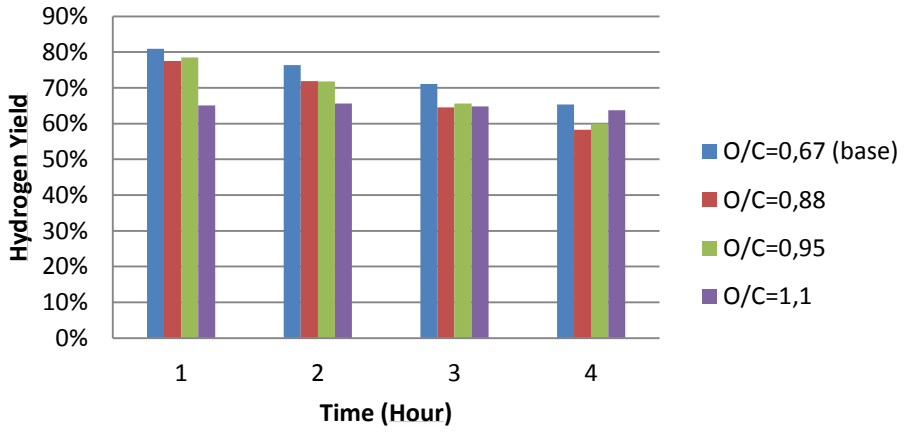

(c)

FIGURE 9 Hourly (average) hydrogen yield during steam reforming of pyrolysis oil aqueous fraction at 650°C using (a) Reformax, (b) Zirconia monolith + Reformax and (c) VTT's Ni/ZrO_2 catalyst in different O/C ratios

6.3 Product Gas Profile

The stability of C2G conversion and hydrogen production can also be seen from the product gas profile recorded by the real time gas analyser. There were 5 gases monitored continuously and their concentration were recorded every 30s mean interval, which are CO. CO_2, CH_4, H_2 and O_2. These data can also be used to see the profile for each gas and their conversion behaviour during the reaction. Figure 10 shows the product gas profile for each type of catalyst. Note that O_2 was totally consumed during the experiment, thus the concentration is not included in the figures.

From Figure 10, it can be seen that each catalyst had its own product gas concentration characteristics. Reformax (Fig. 4a) shows constant CO and CO_2 concentrations, while there was a slight increase for CH_4 and slightly stronger decrease in H_2 production. Addition of zirconia monolith (Fig. 4b) shows almost the same tendency for CO, CO_2 and CH_4 profiles during the experiment. However, there was a significant difference in H_2 concentration. In comparison with stand-alone Reformax, the production of H_2 remained more stable during the experiment when zirconia monolith was added. Combination of zirconia monolith and Reformax also resulted in hydrogen production maximum in later time, not in the beginning of the experiment.

VTT's Ni/ZrO_2 catalyst shows totally different product gas profiles, with a noticeable increase in CO and CH_4 concentrations. Meanwhile, CO_2 was decreasing over time significantly and a rapid decrease of H_2 was recorded during the experiment. The profiles for other O/C ratios indicate the same tendencies of product gas composition. The full figures can be seen in Appendix C.

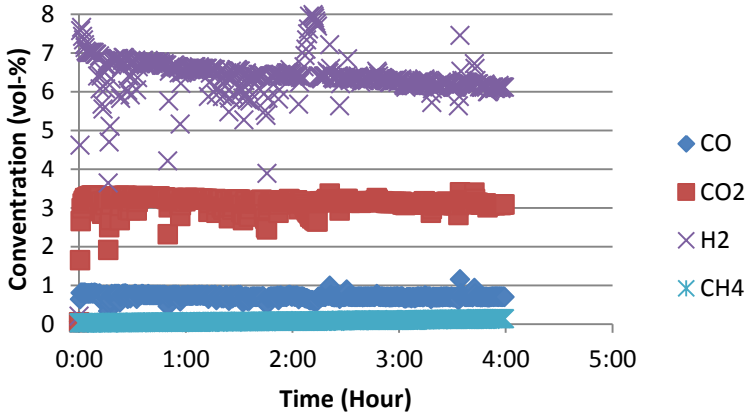

(a)

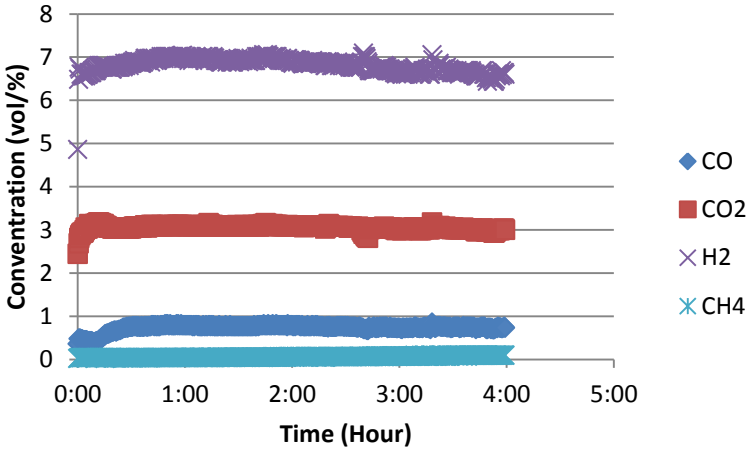

(b)

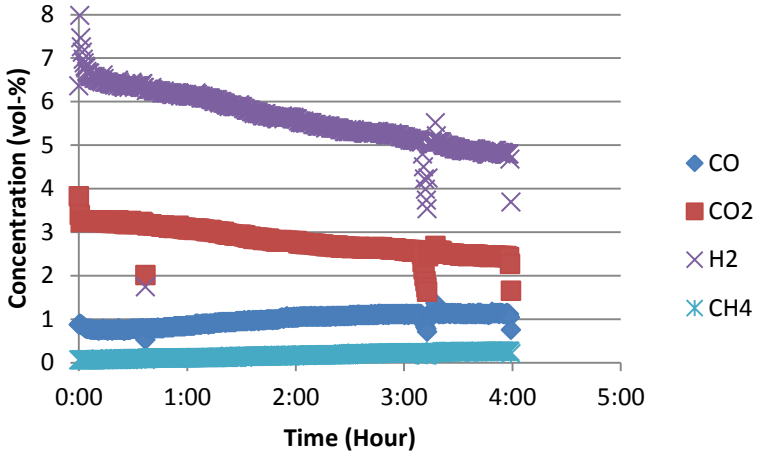

(c)

FIGURE 10 Product gas profile during the experiment of steam reforming of pyrolysis oil aqueous fraction at 650°C, O/C ratio 0,95 using (a) Reformax, (b) Zirconia monolith + Reformax and (c) VTT Ni/ZrO_2 catalyst

6.4 C_2Formation of C_2 Compounds

Beside the real time gas analysis, GC analysis was conducted several times during each experiment. The purpose of the analysis was to follow the formation of C2 compounds. Figure 11 shows an example of ethene (C_2H_4) formation trend-lines indicated for each catalyst used.

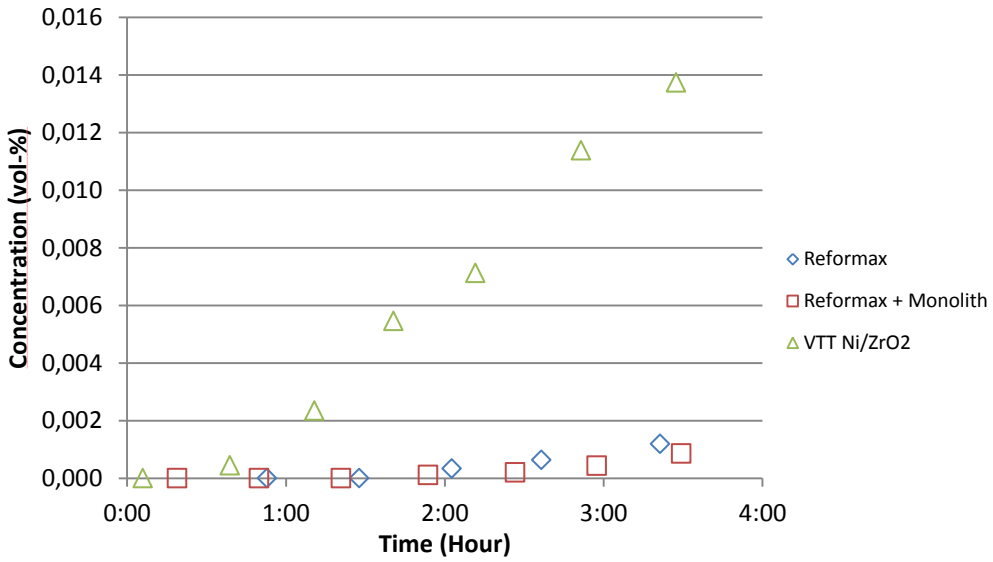

FIGURE 11 Ethene (C_2H_4) production during steam reforming of pyrolysis oil aqueous fraction at 650°C, O/C ratio 0.95, using different catalysts and catalysts combinations

From Figure 11, it can be seen that each catalyst had different trends of ethene production. During 4 hours of reaction, ethene started to form between the 1st and 2nd hour when Reformax catalyst was used. Addition of zirconia monolith to the system showed a slight suppression of ethene formation. Meanwhile, use of VTT's Ni/ZrO_2 catalyst led to more rapid formation of ethene during the reaction. Note that all ethene production curves in Figure 11 still show increasing trends when the experiments were terminated regardless the catalyst being used.

Other C2 compounds that were monitored during the experiments using GC were ethane (C_2H_6) and ethyne (C_2H_2). Both compounds showed almost similar

trends with ethene production. The complete figures of ethane, ethene and ethyne productions in different O/C ratios can be seen in Appendix C.

6.5 Carbon Deposit

Carbon deposits were formed during the reaction mainly on the wall of reactor's top part and on the catalysts. During the burning, most of the carbon on the catalyst reacted into CO and CO_2, while the wall coke remained. Table 11 shows the carbon deposit amount for each experiment.

TABLE 11 Amount of carbon deposit on catalyst and wall coke retrieved after coke burning

Catalyst	Run	Run Hour	O/C	C2G Conversion (%)	Catalyst Burned Deposit (%)	Wall Coke (%)
NiO Reformax	BAFA-4 (base)	4	0.67	86	5.3	3.6
	BAFA-14	4	0.88	82	4.4	8.6
	BAFA-7	4	0.95	74	6.5	4.0
	BAFA-6	4	1.1	81	2.8	9.4
ZrO2 Monolith + NiO Reformax	BAFA-10 (base)	4	0.67	85	5.3	6.6
	BAFA-12	4	0.88	81	6.7	5.5
	BAFA-13	4	0.95	86	4.6	4.5
	BAFA-18	4	1.1	86	4.4	4.1
VTT's Ni/ZrO2	BAFA-9 (base)	4	0.67	83	7.0	4.1
	BAFA-17	4	0.88	77	6.5	5.3
	BAFA-15	4	0.95	86	6.0	4.1
	BAFA-16	4	1.1	67	2.4	7.3

It can be seen from Table 11 that there is no correlation between type of catalyst used and O/C ratios to the amount of carbon deposit formed, either on the reactor wall or on the catalyst. However, there is an indication of decrease in catalyst deposit in zirconia monolith + Reformax system along with increase of O/C ratio. This pattern does not appear in the result for the other two catalyst systems.

Most of the carbon deposit was formed on the reactor wall near the feeding system (at the top of the reactor). The carbon deposit looked like porous carbon which was predicted to be pyrolytic carbon resulting from exposure of higher oxygenates to high-temperature, which results in thermal decompositions [25]. This phenomenon was quite severe and sometimes it was limiting the reaction due to high pressure trapped inside the reactor when the wall coke started to clog the system. Figure 12 shows the carbon appearances on the wall, feeding system and burned catalyst.

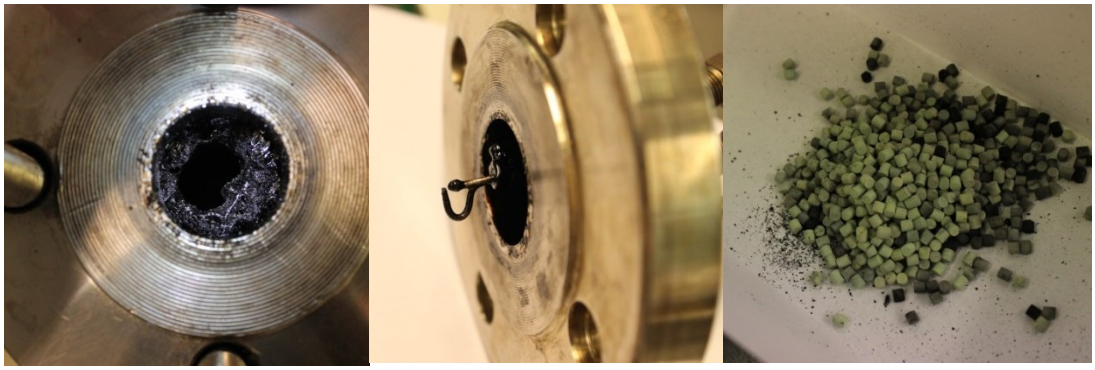

(a) (b) (c)

FIGURE 12 Appearance of (a) wall coke on top of the reactor, (b) coke on the sprayer and (c) carbon deposit on burned catalyst

7. Discussion

7.1 Effects of Catalyst

7.1.1 Effects of Catalyst on Carbon-to-Gas Conversion

From section 4.1, Reformax and combination of zirconia monolith + Reformax show better C2G stability compared to VTT Ni/ZrO_2 catalyst. Both systems consistently provided C2G conversions above 80%, except for BAFA-7, which also indicates anomaly between the other variations. Generally speaking, Reformax and VTT's Ni/ZrO_2 systems have the same WHSV, while the combination of zirconia monolith + Reformax has a different one. This might be one reason why the catalyst combination resulted in more consistent C2G conversion for all the O/C variations.

Lower WHSV in this combination system was achieved due to same amount of Reformax as the stand alone one was used, added with approximately 15 grams of zirconia monolith. This lower WHSV provides longer time for the feedstock to react, both for main or secondary reactions. Therefore, chance of the feedstock to be converted into smaller gaseous compounds is higher, resulting in better C2G performance for the combination system of zirconia monolith + Reformax.

Another reason that can be correlated to the result is the catalytic performance of zirconia monolith. It was previously investigated by VTT that zirconia monolith can decompose tars and heavier compounds in gasification gas cleaning [38, 47]. Although the activity of this catalyst towards pyrolysis oil aqueous fraction has not been investigated, it looks like zirconia plays a role in helping the conversion of heavy compounds into smaller compounds that are easier to be further reformed into gases.

It is hard to take any conclusion about effects of the catalyst to the C2G conversion due to some technical issues. Clogging in the feeding system was one of the causes of uncertainty. It was observed that during the experiment, sometimes the whole product gases concentration went down for several moments before went up and stabilize again. It was also observed that the gas flow for each run did not show almost the same value, sometimes it had significant differences. This fluctuation might be resulted from occasional problem in feeding system that occurred due to natural flow properties of the feedstock.

7.1.2 Effects of Catalyst on Hydrogen Production

In terms of hydrogen production, Reformax and combination of zirconia monolith + Reformax exhibited higher hydrogen production rate compared to VTT's Ni/ZrO_2. Both catalysts showed a comparable overall result regardless the O/C ratio used, indicated by almost overlapping graphs on Figure 8. However, addition of zirconia monolith as a pre-reformer catalyst resulted in better production stability. Based on Figure 3a and 3b, with every O/C ratio, combination of zirconia monolith + Reformax exhibited remarkably more stable hydrogen yields during the 4 hour experiment. The lower WHSV of combination system might also help to provide enough time and chance for the reforming reactions to take place.

Just like the case of C2G conversion, zirconia monolith might play a role in decomposing heavy compounds into smaller and easier to reform compounds that results in better hydrogen yield. Furthermore, the pre-reformer catalyst might also help by acting as catalyst of selective oxidations, which leads to oxidation of non-hydrogen compounds (CO, CH_4, C2 compounds, etc.). This hypothesis is also reinforced by the fact that C2 formation was supressed when zirconia monolith was added to the system and the CH_4 concentration in the outlet gas of combination system was slightly lower than other catalyst systems.

On the other hand, Ni/ZrO_2 system had the lowest hydrogen yield and also stability. This catalyst has unique product gas profiles where CH_4 concentration was observed to increase quite significantly during the experiment. Moreover, this in-house made catalyst also promoted C2 compounds formation faster than the other two catalysts. These tendencies also explain why the hydrogen yield decreased fast. Hydrogen might be consumed in the formation of CH_4 and C2 compounds that show rapidly increasing profiles compared to the other compounds during the experiments.

One interesting phenomenon in this experiment was the decreasing hydrogen profile for each catalyst with all different O/C ratios. Despite the technical issue in the experiments, Reformax and Ni/ZrO_2 catalysts showed more significant and irregular decreases of overall hydrogen yield over higher O/C ratios. Meanwhile, combination of zirconia monolith + Reformax showed more steady, patterned and mild decreases. This might also be because the role of zirconia monolith as pre-reformer that stabilized the system by turning the feed into lighter and easier-to-react compounds before it reached the main reforming catalyst.

7.2 Effect of O/C Ratio

7.2.1 Effect of O/C Ratio on Carbon-to-Gas Conversion

As mentioned in section 4, the O/C ratio gives several positive effects on stabilizing the C2G conversion. It was observed for systems with Reformax and VTT Ni/ZrO_2 catalysts, that C2G conversions stability was better at higher O/C ratios. This phenomenon can be explained by more exothermic reaction taking place in the system during addition of oxygen. With more exothermic reactions happening, heat can be supplied more evenly in the reaction, resulting in faster and more stable kinetics. It also provides better heat transfer due to more evenly distributed and steadier temperature inside the reaction zone. Thus, more stable conversion values can be achieved compared to system without presence of additional oxygen.

In the case of VTT's Ni/ZrO_2 catalyst, higher oxygen content stabilized the hourly C2G conversions at O/C ratio 1.1. With lower O/C ratios, the conversion peaks started immediately during the first hour, but then they decreased significantly during the experiment. However, at the highest O/C ratio, the conversion remained stable for 4 hours. This result can be a clear indication of the role of oxygen in improving the C2G conversion stability. One possible reason is that oxygen promotes oxidation, partial oxidation or breaking of higher-chained hydrocarbons that cannot be reformed easily by the catalyst, leading to a stable C2G conversion. The second possible reason is oxygen helps in regenerating the catalyst by continuously burning part of the carbon deposit on the catalyst surface, resulting in more stable catalyst activity and C2G conversion. Note that these phenomena can also happen in the other catalyst systems or in different O/C ratios. However, the conversion decrease might start in later time or in a lower rate; thus the pattern could not be seen during the 4 hour experiment time-on-stream.

7.2.2 Effect of O/C Ratio on Hydrogen Production

The experimental results in hydrogen production are in line with the theory related to it. With addition of oxygen, more hydrogen will be oxidized; therefore the amount of hydrogen produced will decrease upon increase of O/C ratio. Figure 8 shows this comparison clearly, where with all catalyst systems increase of O/C ratio resulted in lower hydrogen production and the stoichiometric maximum values could not really be reached due to kinetic limitations.

Regarding hydrogen yield stability, there is an indication of positive involvement of oxygen in stabilizing the hydrogen yield over time. In all catalyst system, there is a tendency of more stable hydrogen yield with higher oxygen addition. Although the differences are small (1-2% improvements) and might be in the range of measurement error, the indication is quite clear for Ni/ZrO_2 system. At the highest O/C ratio of 1.1, the hydrogen yield remains pretty stable in

comparison with the lower O/C ratio ones. This positive effect of oxygen can be possibly explained with the same reasons as for better C2G conversion. Addition of oxygen might help in regenerating part the catalyst continuously during the operation—resulting in longer catalyst activity—and also breaking longer-chained hydrocarbons that leads to better reforming performance.

7.3 Total Carbon Balance

The total carbon balance that was calculated for all the experiment variations did not reach 100% accuracy. There are several reasons that can be taken into consideration while discussing about this matter.

In this system, the carbon loss might occur due to different reasons. Firstly, the total carbon balance did not include C2 compounds, which were formed and appeared in the GC analysis. This was done due to limitation in providing continuous data about C2 compounds that cannot be observed real time, unlike the other gases. GC analysis also sometimes showed unknown peaks which might be unknown carbon compounds. Moreover, the GC analysis was limited until compounds with retention time no longer than 20 min. This resulted in probability of several higher-than-C2 compounds to be undetected.

The second possible reason is unburnt carbon or coke. During the experiment and after the coke burning, several carbon and coke remained unburnt and becoming very fine and light particles. These particles were hard to collect—and to weigh—and were also creating black layers on the hoses, which were not measured.

Another possible explanation for carbon mass loss is leakage. Although pressure test was conducted before each experiment, the gas leakage sometimes could not be avoided. The most frequent one was during the GC sampling when the pressure of the system was increased purposely to make sure the gas was running to the GC line. At some rate, the gas cleaning system, which was iso-

propanol and water line in glass jars, sometimes could not afford the pressure and opened for a very short time. This event was followed by short pressure drop in the system and a popping sound from the glass jars. Personal gas detector was also able to notice the leakage for several times.

The carbon balance also affected the hydrogen production. Based on the result in Section 4, the hydrogen production was following the theory—the hydrogen production goes down as the O/C ratio increases. From Figure 8, it can be also seen that the graph follows the trend-line of theoretical calculation. Since the carbon conversions did not reach total conversion, there were gaps between theoretical maximum production and experimental results. This is the main explanation why hydrogen did not reach it theoretical maximum values.

Other reason why hydrogen did not reach the maximum stoichiometric value can be explained by several technical reasons, such as leakage which result in direct hydrogen loss due to release of the compound to the environment, which cannot be detected. Furthermore, hydrogen can also react with C, CO and CO_2 to form methane via methanation reactions. Some catalyst might also promote these reactions, such as Ni/ZrO_2 that showed increase in CH_4 production during the experiment over time. H_2 can also be trapped in C2 compounds that were not reformed or react back with smaller compounds to form C2 or higher hydrocarbon compounds. Furthermore, there might be also small fraction of hydrogen solute in the water bath of gas cleaning system. However, these loses coped only small amount of hydrogen loss.

7.4 Formation of C2 compounds

The C2 compounds formation is another interesting phenomenon in this experiment. Ni/ZrO_2 catalyst seems to promote C2 compound formations while addition of zirconia monolith to the Reformax system tends to supress the C2 compound formations. Based on Figure 19-21 in Appendix C, ethane and ethene were produced more when Ni/ZrO_2 catalyst was used regardless the O/C ratios,

while ethyne rarely appeared significantly during the experiments. However, in all experiments the amounts of C2 compounds were still increasing even at the end of the runs. Thus, it cannot be simply concluded whether the fast formation and the slow formation are also correlated to the maximum value of the formation for each C2 compound. It is not impossible that at particular time for each system, the same amounts of C2 compounds are stabilized. One possible reason for the unachieved maximum value is catalyst deactivation, which leads to lower conversion of higher-chained hydrocarbon (in this case, C2 compounds). Therefore, longer and more intensive research might be a good idea to see this phenomenon more clearly and insightful.

7.5 Long Term Run

The long term run was conducted to further see the stability of the catalysts. Experimental conditions with O/C ratio = 0.95 using zirconia monolith + Reformax catalysts were chosen. These conditions were chosen since they represent addition of oxygen to the system and zirconia monolith had proven its benefit after all variations were investigated. This variation also achieved good C2G conversion and total carbon balance. The result for C2G conversion and hydrogen yield can be seen in Figure 13. The long term run lasted for more than 15 hours, however, only first 14 hours of data were representative and presented here.. The overall C2G conversion was 75% and hydrogen yield of 62%. Figure 13 shows that the conversion and hydrogen yield decreased during the 14 hours' time lapse. The first 4 hours of the run were comparable with BAFA-13, which had the same process conditions. After relatively stable period, the decrease of both C2G conversion and hydrogen yield started to get more rapid after 10 hours' time-on-stream. The most rapid decrease occurred during the 12-13 hours, both for C2G conversion and hydrogen yield. Based on this result, the 4 hours run might not be able to fully represent the long term result of each system in the main experiments.

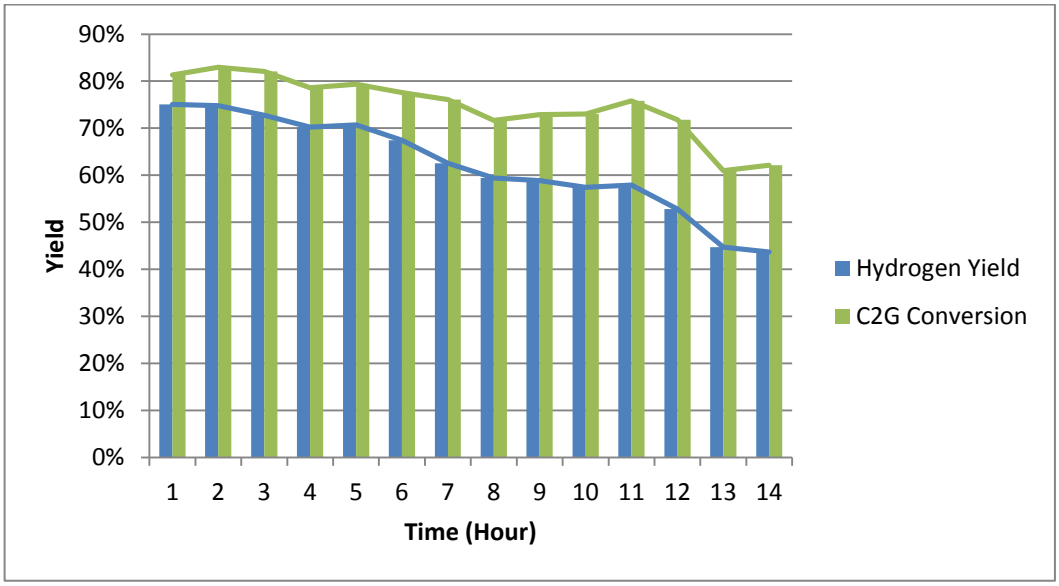

FIGURE 13 Hourly average carbon-to-gas and hydrogen yield for long term experiment of oxidative steam reforming of pyrolysis oil aqueous fraction at 650°C, O/C = 0.95 using zirconia monolith + Reformax catalysts

The run was cut after 15 hours not due to the catalyst deactivation but because the pressure drop over the reactor was too high—indicating a blockage of flow in the reactor mainly caused by wall coke. Thus, the total deactivation of the catalyst could not be detected by this experiment. As the main problem was wall coke, design of reactor and feeding system are the main challenges for long term run and will be further discussed in the next section.

During the experiment, some shut downs were conducted for feeding system cleaning purposes. The cleaning was necessary due to findings in 4 hour experiments where the sprayer was sometimes blocked after the run. There were two cleaning periods and when the reactor was starting up again, the gas product profile could reach almost the same stable state as before the reactor was turned off although it took time. This indicated that the catalyst was not affected significantly by the cleaning procedure.

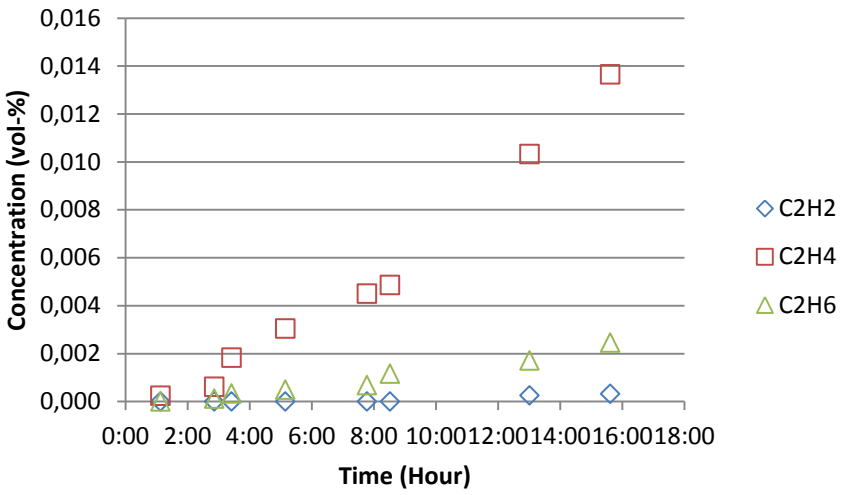

FIGURE 14 C2 compounds profile in the product gas of oxidative catalytic reforming of pyrolysis oil aqueous fraction at 650°C, O/C = 0.95, using zirconia-monolith catalysts

The C2 compounds were also being investigated to see if there was any peak or stable C2 compounds profile achieved. However, based on Figure 14, there was no indication of stable production of C2 compounds or peak production even after more than 15 hour time-on-stream.

The catalysts were not subject to burning procedure after the experiment. Figure 15 shows the catalyst condition and the wall coke retrieved from the top of the reactor. The wall coke amount corresponded to 15% of the whole carbon being fed to the system, indicating huge carbon loss due to wall coke formation. The wall coke was found to be 12 times higher than the carbon formed in the same system running for 4 hours (BAFA-13). This phenomenon clearly indicated that the feeding system and the whole reactor design were not fully compatible for pyrolysis oil aqueous fraction reforming, especially for long term experiment.

7.6 Reactor Design and Feeding System

The reactor used in this study was an improvement of Sánchez (2013) equipment. The main improvement was in the feeding system. Albeit the sprayer

was still easily being moved and not completely fixed, it was designed to handle the pyrolysis oil aqueous fraction pretty well. The vibration that was experienced by Sánchez was solved by attaching gas and water line in the feeding system tightly, resulting in more solid spraying patterns. This resulted in no further feeder changes during the whole study and no severe clogging in the sprayer line as often occurred in Sánchez [42] experiments. The clogging in the line can easily be removed by normal cleaning using methanol or ultrasound cleaner for 20 minutes.

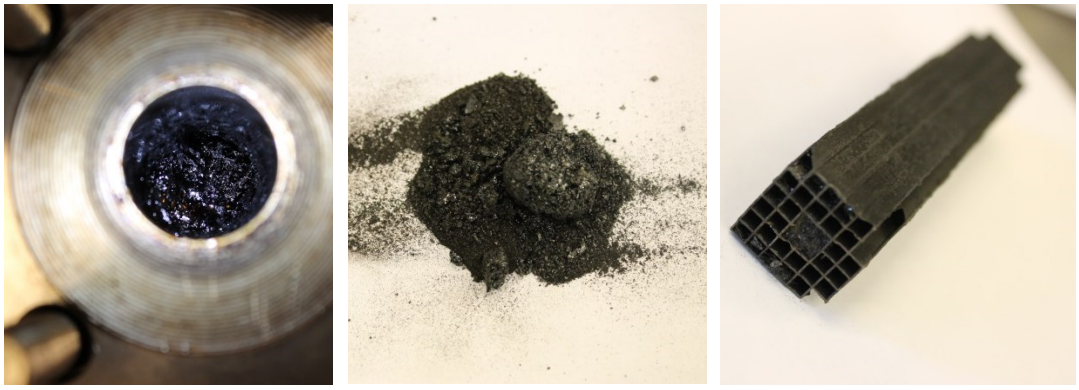

(a) (b) (c)

FIGURE 15 16 Appearance of (a) wall coke on top of the reactor, (b) retrieved wall coke (c) carbon deposit on unburned monolith catalyst after long run experiment of oxidative steam reforming of pyrolysis oil aqueous fraction at 650^{o}C. O/C=0.95 for ~15 hours

However, the configuration of the feeding system still allowed the feed to reach some empty part of the reactor and not directly sprayed onto the catalyst, resulting in wall coke at the top of the reactor. It was observed that the amount of wall coke varied between 35-80% of the total carbon deposit measured in each experiment. This wall coke formation was the most severe problem and it proved to limit the long term experiment due to total clogging of the reactor top before the catalyst was completely deactivated. Thus, fixed bed configuration with sprayer was not the best choice for this experiment. This was in line with Czernik et al.[34], Kechagiopoulos et al. [35] and Sánchez [42] that fixed bed reactor was not suitable for catalytic steam reforming of pyrolysis oil or its

aqueous fraction since it mostly resulted in fast catalyst deactivation, reactor clogging and coke formation in the nozzle system. Therefore, the reactor design for this system might be further evaluated. Several researchers suggested that fluidized bed reactor can be a better option [34, 42, 43] as it gives better contact between reactant, steam and catalyst, and temperature gradient present in the fixed bed reactor is avoided.

8. Conclusions and Recommendations

Based on literature review, the steam reforming process of pyrolysis oil is still developing, immature and faces big challenges to be implemented, especially in large scale. Furthermore, the problems related to reactor design and feeding system are the main challenges for development of this process, where mainly limiting the study of the catalyst testing itself. On the other hand, several commercial catalysts have shown show promising results—mainly nickel based catalysts—which open a good opportunity for further investigation of this technology despite several limitations in activity and catalyst coking.

Based on the experimental results, commercial nickel based catalyst (Reformax) showed a good performance with C2G conversion above 70% with all tested O/C ratios, despite the fact that S/C ratio was relatively low (3.84) compared to previous experiments. Addition of zirconia monolith was a good breakthrough to reach more stable conversion, achieving carbon-to-gas conversion above 80% when combined with nickel based catalyst. Addition of zirconia monolith also gave promising result in providing more stable hydrogen yield compared to stand-alone nickel catalyst system. Furthermore, it was also indicated that zirconia monolith suppress the formation of C2 compounds side products which lower the overall hydrogen production amount. This result was opposite to the study by Sánchez (2013) where it was stated that zirconia monolith did not show any beneficial effect with the same feedstock and system configuration.

Addition of oxygen via feeding of air was proved to stabilize both C2G conversion and hydrogen production, despite the fact that it lowered the overall hydrogen yield. Each catalyst or catalyst combination seemed to have a particular minimum oxygen addition amount affecting stable C2G conversion and hydrogen production rate.

The main challenge in this study was related to the reactor design and feeding system which caused severe wall coke formation that blocked the reactor and reduced the carbon conversion significantly. Thus, it is recommended for a further study to design a better or a more advanced system before running further tests, by using either fluidized bed or moving the feeding system as close as possible to the catalyst bed to avoid feed decomposition and polymerization before it reaches the catalytic region. Furthermore, it is also recommended to run tests with longer time-on-stream as the long term run showed an interesting behaviour after 4 hours running, where the deactivation seemed to accelerate. It is also worthwhile to run long term tests to investigate the C2 formation profile in depth. Other recommendations for further studies are investigation of the role of zirconia monolith to the particular feedstock to see how it benefits the whole system and development of a reinforced Ni/ZrO_2 catalyst, which showed good initial results but with really fast deactivation rates.

References

[1] Tumurulu JS, Sokhansanj S, Wright CT, Boardman RD. 2010. Biomass torrefaction process review and moving bed torrefaction system model development. INL, USA.

[2] Bridgwater AV. 2012. Review of fast pyrolysis of biomass and product upgrading. Biomass and Bioenergy 38, pp. 68-94.

[3] Basu P. 2010. Biomass Gasification and Pyrolysis - Practical Design and Theory, Oxford: Elsevier, pp. 65-92.

[4] Bridgwater AV. The production of biofuels and renewable chemicals by fast pyrolysis of biomass. International Journal of Global Energy Issues, 2007, vol. 27, pp. 160-203.

[5] Czernik S, Bridgwater AV. 2004. Overview of applications of biomass fast pyrolysis oil. Energy Fuels 18, pp. 590–598.

[6] Mohan D, Charles U, Steele PH. 2006. Pyrolysis of wood/biomass for bio-oil: a critical review. Energy Fuels 20, pp. 848–889.

[7] Vitasari CR, Meindersma GW, de Haan AB. 2011. Water extraction of pyrolysis oil: The first step for the recovery of renewable chemicals. Bioresource Technology 102, pp. 7204-7210.

[8] Sipilä K, Kuoppala E, Fagernäs L, Oasmaa A. 1998. Characterization of biomass based flash pyrolysis oils. Biomass and Bioenergy 14, pp. 103–113.

[9] Bridgwater AV, Peacocke GVC. 2000. Fast pyrolysis processes for biomass. Renewable & Sustainable Energy Reviews 4, pp. 1–73.

[10] Oasmaa A, Leppämäki E, Koponen, P, Levander J, Tapola E. 1997. Physical Characterization of Biomass-Based Pyrolysis Liquids: Application of Standard Fuel Oil Analyses. Report, VTT Publication 306.

[11] Oasmaa A, Solantausta Y, Arpiainen V, Kuoppala E, Sipilä K. 2010. Fast pyrolysis bio-oils from wood and agricultural residues. Energy Fuels 24, pp. 1380-1388.

[12] Venderbosch RH, Prins W. 2010. Fast pyrolysis technology development. Biofuels Bioproducts and Biorefing 4, pp. 178-208.

[13] Zhang SP, Li XJ, Li QY, Xu QI, Yan YJ. 2011. Hydrogen production from the aqueous phase derived from fast pyrolysis of biomass. Journal of Analytical and Applied Pyrolysis 92, pp. 158-163.

[14] Aho A, Salmi T, Murzin DY. 2013. The role of catalysis for the sustainable production of bio-fuels and bio-chemicals, Chapter 5: Catalytic pyrolysis of lignocellulosic biomass. Elsevier, pp. 137-159.

[15] Huber GW, Iborra S, Corma A. 2006. Synthesis of transportation fuels from biomass: chemistry, catalysts, and engineering. Chemical Reviews 106, pp. 4044-4098.

[16] Aho A, Tokarev A, Backman P, Numar N, Eränen K, Hupa M, Holmbom B, Salmi B, Murzin DY. 2011. Catalytic pyrolysis of pine biomass over H-beta zeolite in a dual-fluidized bed reactor: effect of space velocity on the yield and composition of pyrolysis products. Topics in Catalysis 54, pp. 941-948.

[17] Haynes DJ, Shekhawat D. 2011. Fuel Cells: Technologies for fuel processing, Chapter 6: Oxidative steam reforming. Elsevier, pp. 129-190.

[18] Qi A, Wang S, Fu G, Wu D. 2005. Autothermal reforming of n-octane on Ru-based catalysts. Applied Catalysis A: General 293, pp. 71-82.

[19] Borup RL, Inbody MA, Semelsberger TA, Tafoya JI, Guidry DR. 2005. Fuel composition effects on transportation fuel cell reforming. Catalysis Today 99, pp. 263-70.

[20] Ahmed S, Krumpelt M. 2001. Hydrogen from hydrocarbon fuels for fuel cells. International Journal of Hydrogen Energy 26, pp. 291-301.

[21] Lindermeir A, Kah S, Kavurucu S, Mühlner M. 2007. On-board diesel fuel processing for an SOFC—APU—Technical challenges for catalysis and reactor design. Applied Catalysis B: Environmental 70, pp. 488-497.

[22] Wang R, Rohr D. Natural gas processing technologies for large scale solid oxide fuel cells. General Electric Company.

[23] Jones G, Jakobsen JG, Shim SS, Kleis J, Andersson MP, Rossmeisl J, et al. 2008. First principles calculations and experimental insight into methane steam reforming over transition metal catalysts. Journal of Catalysis 259, pp. 147-160.

[24] Trimm DL. 1999. Catalysts for the control of coking during steam reforming. Catalysis Today 49, pp. 3-10.

[25] Sehested J. 2006. Four challenges for nickel steam-reforming catalysts. Catalysis Today 111, pp. 103-110.

[26] Spivey JJ. 2011. Fuel Cells: Technologies for fuel processing, Chapter 10: Deactivation of reforming catalyst. Elsevier, pp. 285-315.

[27] Bond GC. 1997. The role of carbon deposits in metal-catalysed reactions of hydrocarbons. Applied Catalysis A: General 149, pp. 3-25.

[28] Basu P. 2010. Biomass gasification and pyrolysis: Practical design and theory. Elsevier.

[29] Jenkins BM, Baxter LL, Miles Jr. TR, Miles TR. 1998. Combustion properties of biomass. Fuel Processing Technology 54, pp. 17-46.

[30] Rostrup-Nielsen J, Christiansen L. 2011. Concepts in Syngas Manufacture, London: Imperial College Press 10, pp. 213-273.

[31] He et al. 2013. Renewable hydrogen technologies: Production, purification, storage, applications and Safety, Chapter 6: Hydrogen from biomass: Advances in thermochemical processes. Elsevier, pp. 111-133.

[32] Broutin P. 2010. CO_2 Capture, Chapter 5: Pre-combustion CO_2 capture. Editions Technip, pp. 111-139.

[33] Wang D, Czernik S, Montané D, Mann M, Chornet E. 1997. Biomass to hydrogen via fast pyrolysis and catalytic steam reforming of the pyrolysis oil or its fractions. Industrial & Engineering Chemistry Research 36, pp. 1507-1518.

[34] Wang D, Czernik S, Chornet E. 1998. Production of hydrogen from biomass by catalytic steam reforming of fast pyrolysis oil. Energy & Fuels 12, pp. 19-24.

[35] Kechagiopoulos PN, Voutetakis SS, Lemonidou AA, Vasalos IA. 2007. Sustainable hydrogen production via reforming of ethylene glycol using a novel spouted bed reactor. Catalysis Today 127, pp: 246-255.

[36] Hu X, Lu G. 2009. Investigation of the steam reforming of a series of model compounds derived from bio-oil for hydrogen production. Applied Catalysis B: Environmental 88, pp. 376-385.

[37] Ross J. 2012. Heterogeneous Catalysis, Chapter 4: Catalysis preparation. Elsevier, pp. 65-96.

[38] Juutilainen SJ, Simell PA, Krause OI. 2006. Zirconia: Selective oxidation catalyst for removal of tar and ammonia from biomass gasification gas. Applied Catalysis B: Environmental 62, pp. 82-92.

[39] Aho A, Salmi T, Murzin DY. 2013. The role of catalysis for the sustainable production of bio-fuels and bio-chemicals, Chapter 5: Catalytic pyrolysis of lignocellulosic biomass. Elsevier.

[40] Czernik S, French R, Feik C, Chornet E. 2000. Production of hydrogen from biomass-derived liquids. Proceeding of the 2000 DOE Hydrogen Program Review. NREL.

[41] Matsumura Y, Nakamori T. 2004. Steam reforming of methane over nickel catalysts at low reaction temperature. Applied Catalysis A: General 258, pp. 107-114.

[42] Sánchez CAS. 2013. Steam reforming of pyrolysis bio-oil aqueous fraction for hydrogen production. Aalto University, School of Chemical Technology, Master's Thesis.

[43] Medrano J, Oliva M, Ruiz J, García L, Arauzo J. 2011. Hydrogen from aqueous fraction of biomass pyrolysis liquids by catalytic steam reforming in fluidized bed. Energy 36, pp. 2215-2224.

[44] Wang D, Montan D, Chornet E. 1996. Catalytic steam reforming of biomass-derived oxygenates: acetic acid and hydroxyacetaldehyde," Applied Catalysis A: General 143, pp. 245-270..

[45] Ortiz-Toral PJ, Satrio J, Brown RC, Shanks BH. 2011. Steam Reforming of Bio-oil Fractions: Effect of Composition and Stability. Energy Fuels 25, pp. 3289-3297.

[46] Czernik S, French R, Feik C, Chornet E. 2002. Hydrogen by Catalytic Steam Reforming of Liquid Byproducts from Biomass Thermoconversion Processes. Industrial & Engineering Chemistry Research 41, pp. 4209-4215.

[47] Patent Cooperation Treaty. International Publication Number WO 2012/022988 A1. 2012.

[48] Czernik S, French R. 2014. Distributed production of hydrogen by auto-thermal reforming of fast pyrolysis bio-oil. International Journal of Hydrogen Energy 39, pp. 744-750.

[49] Leijenhorst EJ, Wolters W, Van de Beld L, Prins W. 2013. Autothermal catalytic reforming of pine woon derived fast pyrolysis-oil in a 1.5 kg/h pilot installation: Aspects of adiabatic operation. Fuel Processing Technology 115, pp. 164-173.

[50] Liu S, Chen M, Chu L, Yang Z, Zhu C, Wang J, Chen M. 2013. Catalytic steam reforming of bio-oil aqueous fraction for hydrogen production over Ni-Mo supported on modified sepiolite catalyst. International Journal of Hydrogen Energy 38, pp. 3948-3955.

[51] Kechagiopoulos PN, Voutetakis SS, Lemonidou AA, Vasalos IA. 2006. Hydrogen Production via Steam Reforming of the Aqueous Phase of Bio-Oil in a Fixed Bed Reactor. Energy & Fuels 20, pp. 2155-2163.

[52] Hongyu L, Qingli X, Hanshen X, Yongjie Y. 2009. Catalytic reforming of the aqueous phase derived from fast-pyrolysis of biomass. Renewable Energy 34, pp. 2872-2877.

[53] Bimbela F, Oliva M, Ruiz J, García L, Arauzo J. 2011. Steam Reforming of Bio-Oil Aqueous Fractions for Syngas Production and Energy. Environmental Engineering Science 28/11, pp. 757-763.

[54] Yan CF, Hu EY, Cai CL. 2010. Hydrogen production from bio-oil aqueous fraction with in-situ carbon dioxide capture. International Journal of Hydrogen Energy 35, pp. 2612-2616.

APPENDIX A: Calculation Method & Examples

A.1 Carbon-to-gas conversion

The C2G conversion was calculated using Eq. 24.

$$\text{C2G conversion } = \text{X} = \frac{moles\ of\ C\ in\ the\ product\ gas}{moles\ of\ C\ in\ the\ feed} \times 100\% \quad (24)$$

The product gases that were taken into consideration are CO, CO_2 and CH_4. Moles of carbon in the feed were calculated based on chemical formula of each component presents in the feed (see Table 7), with constant parameters including mass flow of aqueous fraction (0.4 ml/min), density of the aqueous fraction (1.0463 g/ml) and the time of the reaction (240 min). This calculation corresponds to same calculation calculated by Sánchez [42].

Example:

From Table 7, acetic acid ($C_2H_4O_2$) accounts for 11.57 wt-% ($w_{acetic\ acid}$) of the aqueous fraction. The molar weight of acetic acid is ($Mr_{acetic\ acid}$) 60.05 g/mol. The mole of carbon from acetic acid in the feed was calculated using Eq. 25.

$$C_i = {}^{w_i}/_{Mr_i} \times [number\ of\ C\ atom]_i \quad (25)$$

Thus

$$C_{acetic\ acid} = {}^{0.1157}/_{60.5} \times 2 = 0.33853\ {}^{mol_{carbon}}/_{g_{feed}}$$

Applying for the same Eq. 25 to all components in the aqueous fraction and sum them up results in carbon content of 0.0105 mol_{carbon}/g_{feed}. The total carbon during 4 hours of experiment can then be determined.

$Total\ Carbon\ in\ Feed$

$$= 0.0105\ {}^{mol_{carbon}}/_{g_{feed}} \times 0.4 \frac{ml}{min} \times 1.0463 \frac{g}{ml} \times 240\ min = 1.0457\ mol_{carbon}$$

Whereas moles carbon in the product gas was calculated by assuming the product gas was following the ideal gas rule, where the moles of each gas can be calculated by Eq. 26.

$$n = \frac{P \times V}{R \times T} \tag{26}$$

Where:

n = number of moles

P = pressure of the outlet/product gas

V = volumetric flow of the gas

R = universal gas constant (0.082 atm L/mol K)

T = product gas temperature in K

The pressure was rounded to 1 atm, the volumetric flow was measured by flow meter and the temperature was measured with a thermocouple (average found to be 23.4^{o}C = 296.55K). For example purpose, the flow of 2.2 L/min is used.

Example:

$$n = \frac{1\ atm\ \times 2.2\ L/min}{0.082\ atm \frac{L}{mol\ K} \times 296.55\ K} = 0.0905\ \frac{mol_{gas}}{min}$$

For ideal gas, volume fraction equals to molar fraction. As the gas analyser measure the gas in volumetric fraction, it could be considered as molar fraction as well. The measured values from gas analyser were recorded every 30s for reduction and main experiment, while sometimes for burning it was recorded

every 20s. For example purpose, 30s intermittent data of 0.03 vol-% CO_2 as example, the moles of carbon can be obtained as follows.

$$Moles\ of\ carbon = 0.0905 \frac{mol_{gas}}{min} \times 0.03 \frac{mol_{carbon}}{mol_{gas}} \times 0.5\ min = 0.00136\ mol_{carbon}$$

To obtain the total carbon, summation of recorded gas analyser data for 4 hours run was therefore calculated.

To calculate each carbon containing gas yield, Eq. 27 can be used:

$$\mathrm{Y}_i = \frac{number\ of\ carbon\ atom\ in\ i \times moles\ of\ i\ in\ the\ product\ gas}{moles\ of\ C\ in\ the\ feed} \times 100\% \qquad (27)$$

Where i can be CO, CO_2 and CH_4 in this experiment, thus the number of atom carbon in each component is always 1.

Note that this calculation can also be implemented for calculating the burning of carbon deposit, where the sum of CO and CO_2 in the outlet gas was considered as amount burned deposit.

A.2 Hydrogen Yield

The hydrogen yield was calculated with Eq. 28.

$$Y_{H2} = \frac{moles\ of\ H_2 in\ the\ product\ gas}{max.stoichiometric\ moles\ of H_2\ can\ be\ obtained} \times 100\% \qquad (28)$$

The maximum H_2 that can be obtained was correspond to

$$\max H_2 = \sum_i \left[(2n + \frac{m}{2} - k)_i \times moles\ of\ i\ compound\ in\ the\ feed \right]$$

Where:

n = number of carbon atoms in molecule i

m = number of hydrogen atoms in molecule i

k = number of oxygen atoms in molecule i

Using this equation, it was obtained that amount of max hydrogen can also be calculated as follows:

$$\max H_2 = \left(2n + \frac{m}{2} - k\right) \times moles\ of\ carbon\ in\ the\ feed$$

Where n, m, k corresponds to empirical formula of organic compounds (where n= 1 and m= 1.44) in the aqueous fraction. For oxidative steam reforming, k also corresponds to O/C ratio that is used (i.e. O/C ratio= 1.1, k= 1.1)

Example:

For O/C ratio= 0.95, the empirical formula of organic compounds is $CH_{1.44}O_{0.95}$. Thus, the max H_2 can be obtained stochiometrically is

$$\max H_2 = \left(2(1) + \frac{1.44}{2} - 0.95\right) {}^{mol_{hydrogen}}/_{mol_{carbon}} \times 0.0105\ {}^{mol_{carbon}}/_{g_{feed}}$$

$$= 0.0186\ {}^{mol_{hydrogen}}/_{g_{feed}}$$

The maximum theoretical hydrogen can be obtained by multiply the value above with total feed being fed. The amount of hydrogen in the gas product was calculated using the ideal gas rule just like in C2G calculation.

APPENDIX B: Intermediate Data

TABLE 12 Intermediate conversion data for each experiment variation

Run	Catalyst	S/C	O/C	Time (h)	Gas Yield (%)				Burned Deposit (%)	Wall Coke (%)
					Y_{H2}	Y_{CO}	Y_{CO2}	Y_{CH4}		
BAFA-4	Reformax	3.84	0.67	4	81	20	64	2	5.3	3.6
BAFA-14	Reformax	3.84	0.88	4	77	18	63	1	4.4	8.6
BAFA-7	Reformax	3.84	0.95	4	68	13	59	1	6.5	4.0
BAFA-6	Reformax	3.84	1.10	4	72	13	66	2	2.8	9.4
BAFA-5	Reformax	3.84	0.88	3	77	17	60	1	-	11.0
BAFA-10	Reformax + Zirconia Monolith	3.84	0.67	4	79	19	65	2	5.3	6.6
BAFA-12	Reformax + Zirconia Monolith	3.84	0.88	4	78	16	65	1	6.7	5.5
BAFA-13	Reformax + Zirconia Monolith	3.84	0.95	4	76	16	68	2	4.6	4.5
BAFA-18	Reformax + Zirconia Monolith	3.84	1.10	4	68	14	69	2	4.4	4.1
BAFA-11	Reformax + Zirconia Monolith	3.84	1.10	4	66	11	61	2	-	-
BAFA-9	VTT's Ni/ZrO2	3.84	0.67	4	83	22	58	3	7.0	4.1
BAFA-17	VTT's Ni/ZrO3	3.84	0.88	4	77	20	54	2	6.5	5.3
BAFA-15	VTT's Ni/ZrO4	3.84	0.95	4	86	21	61	3	6.0	4.1
BAFA-16	VTT's Ni/ZrO5	3.84	1.10	4	67	12	53	2	2.4	7.3

APPENDIX C: Figures and Tables

This appendix contains figures and tables from the results that are not included in the main part of the report.

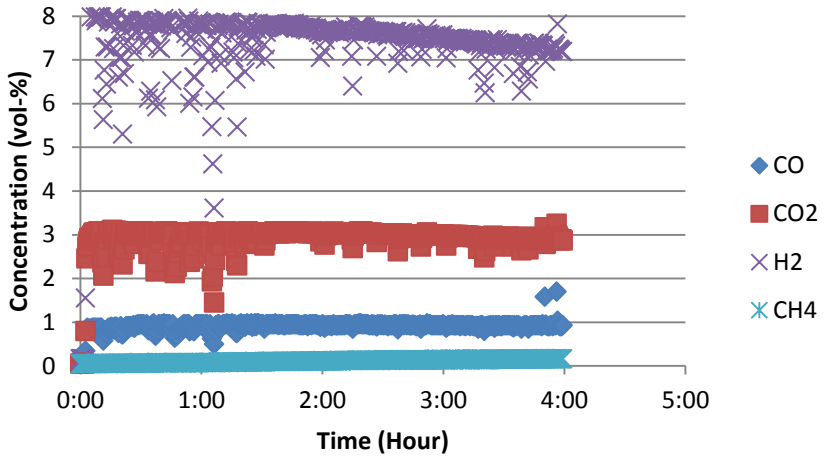

(a)

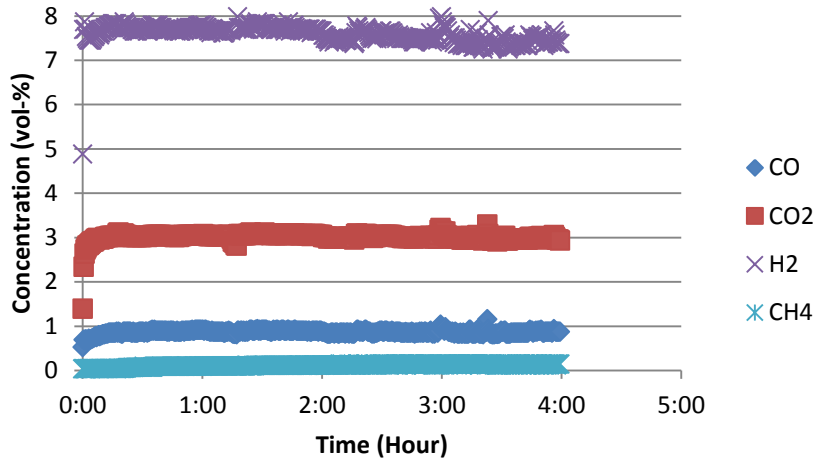

(b)

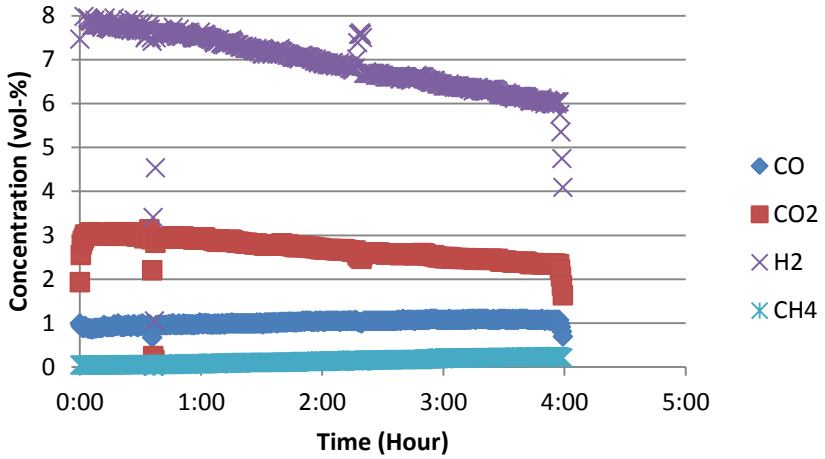

(c)

FIGURE 17 Product gas profile during the experiment of steam reforming of pyrolysis oil aqueous fraction at 650°C, O/C ratio 0.67 (base) using (a) Reformax, (b) Zirconia monolith + Reformax and (c) VTT Ni/ZrO_2 catalyst

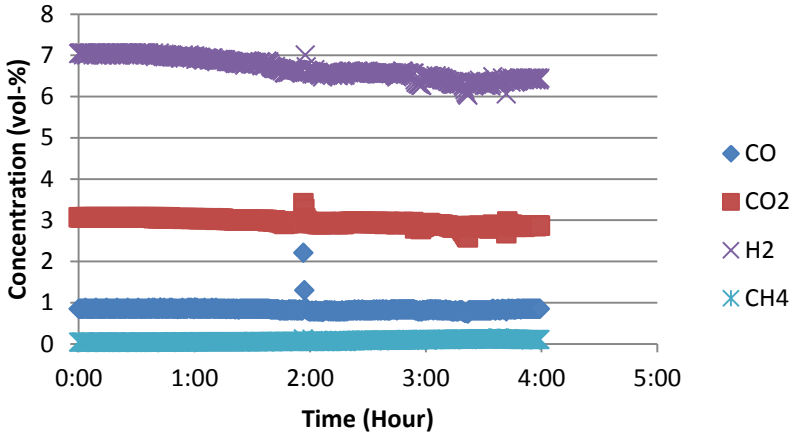

(a)

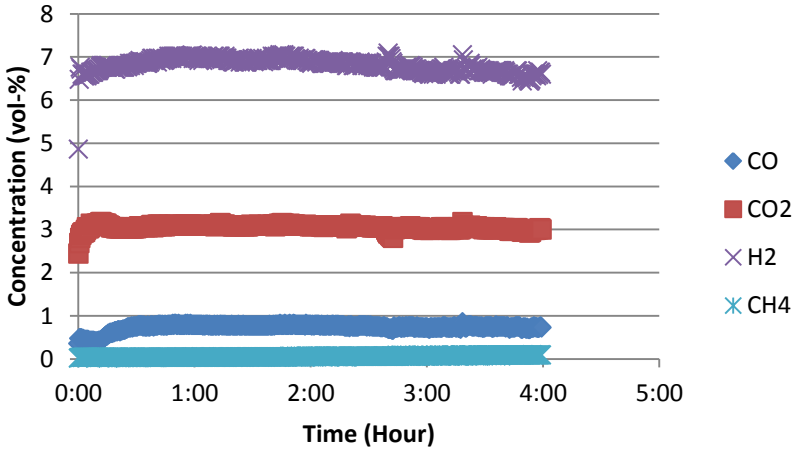

(b)

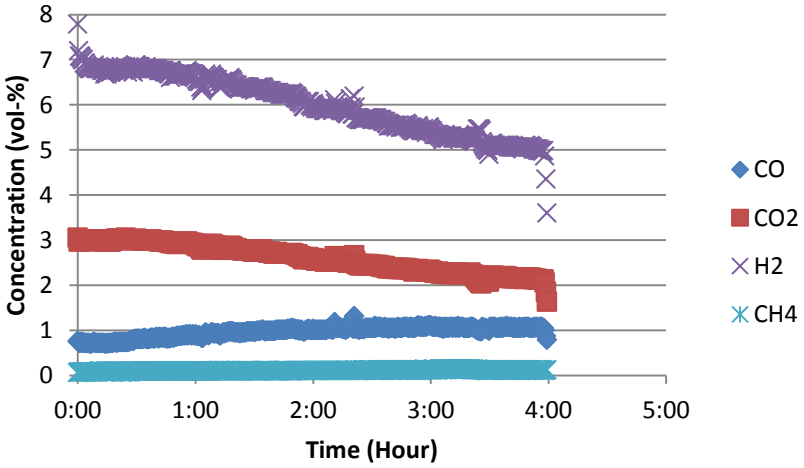

(c)

FIGURE 18 Product gas profile during the experiment of steam reforming of pyrolysis oil aqueous fraction at 650°C, O/C ratio 0.88 using (a) Reformax, (b) Zirconia monolith + Reformax and (c) VTT Ni/ZrO_2 catalyst

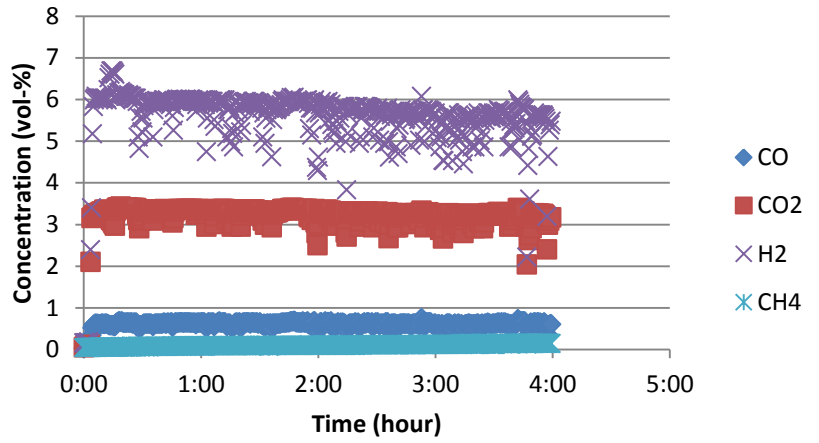

(a)

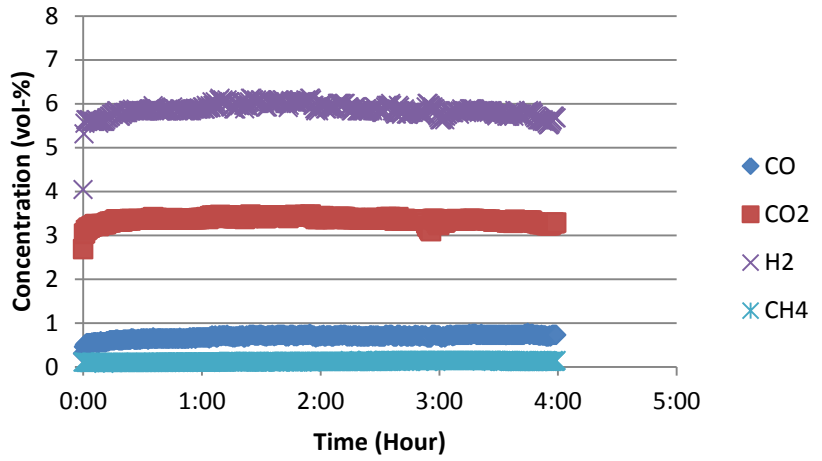

(b)

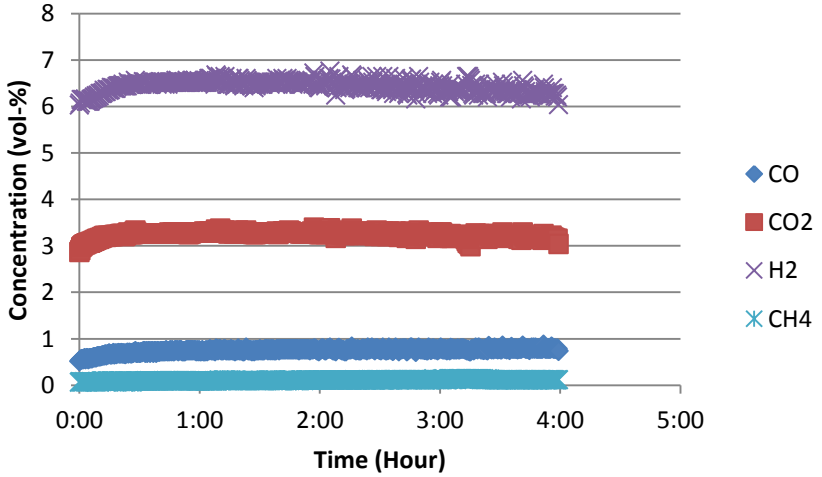

(c)

FIGURE 19 Product gas profile during the experiment of steam reforming of pyrolysis oil aqueous fraction at 650°C, O/C ratio 1.1 using (a) Reformax, (b) Zirconia monolith + Reformax and (c) VTT Ni/ZrO_2 catalyst

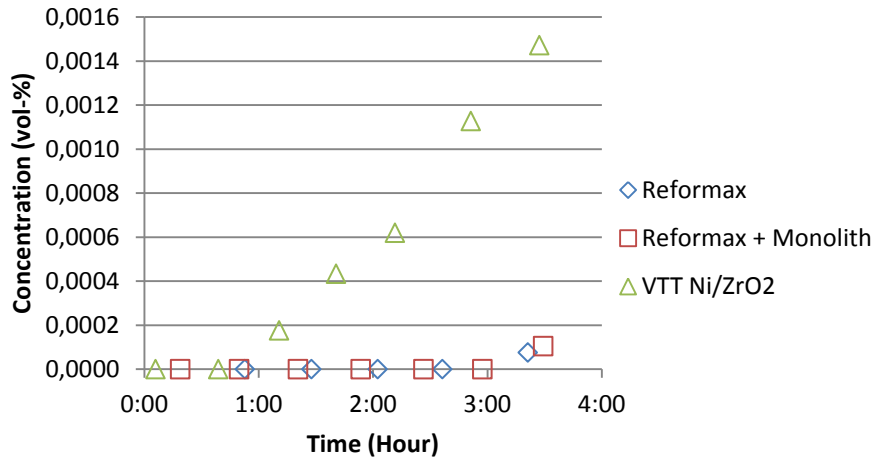

(a)

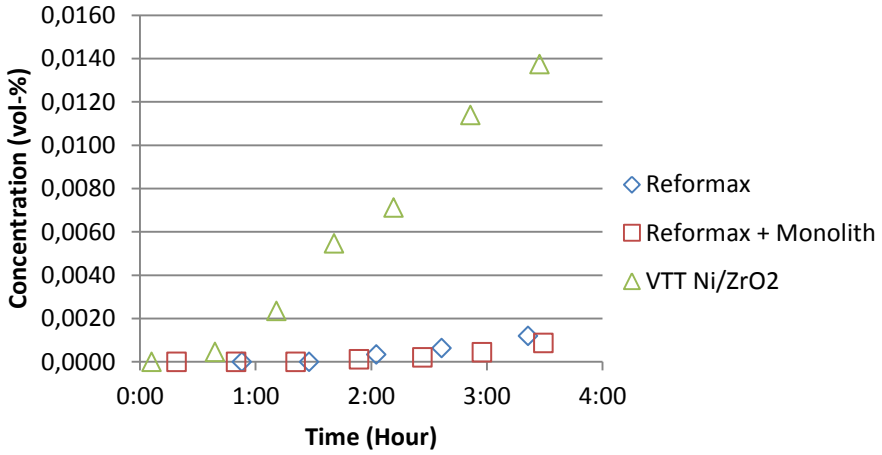

(b)

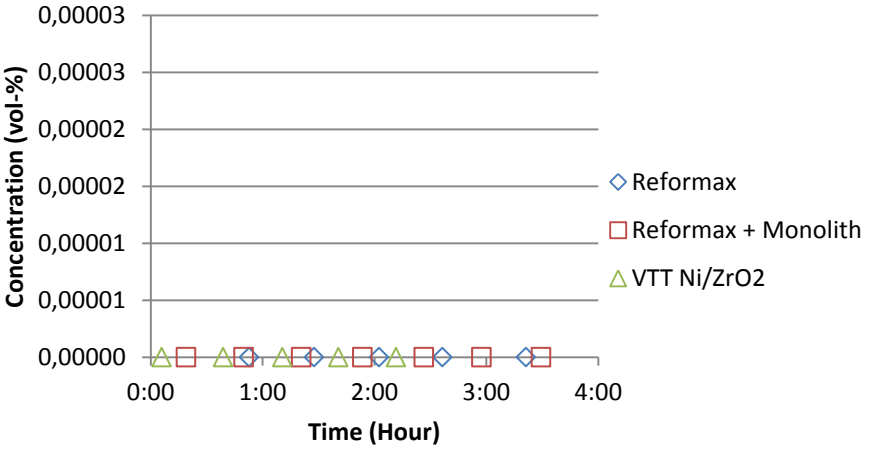

(c)

FIGURE 20 (a) Ethane (C2H6), (b) Ethene (C2H4) and (c) Ethyne (C2H2) production during steam reforming of pyrolysis oil aqueous fraction at 650°C, O/C ratio 0.67, using different catalysts and catalysts combinations

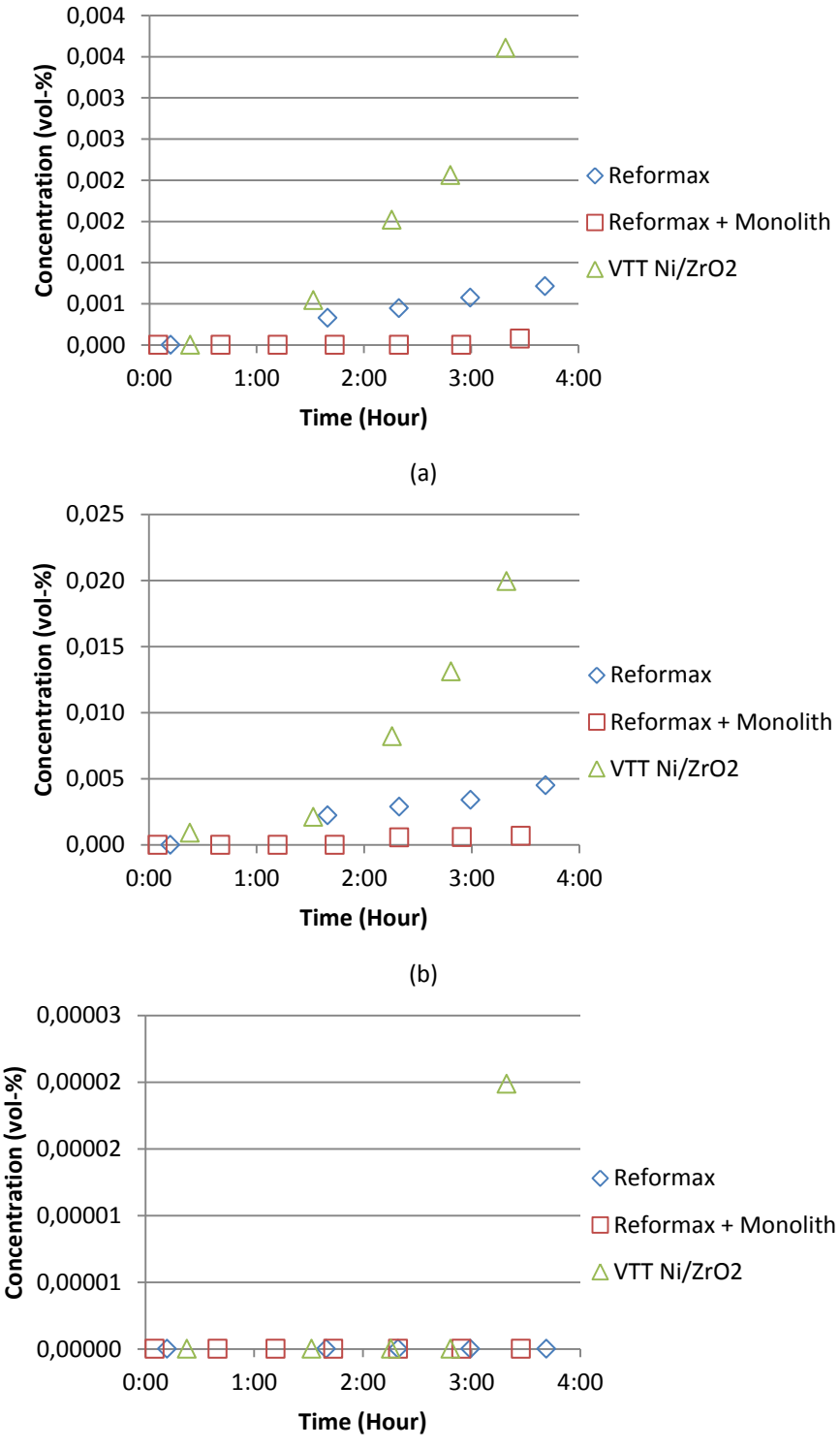

FIGURE 21 (a) Ethane (C_2H_6), (b) Ethene (C_2H_4) and (c) Ethyne (C_2H_2) production during steam reforming of pyrolysis oil aqueous fraction at 650°C, O/C ratio 0.88, using different catalysts and catalysts combinations

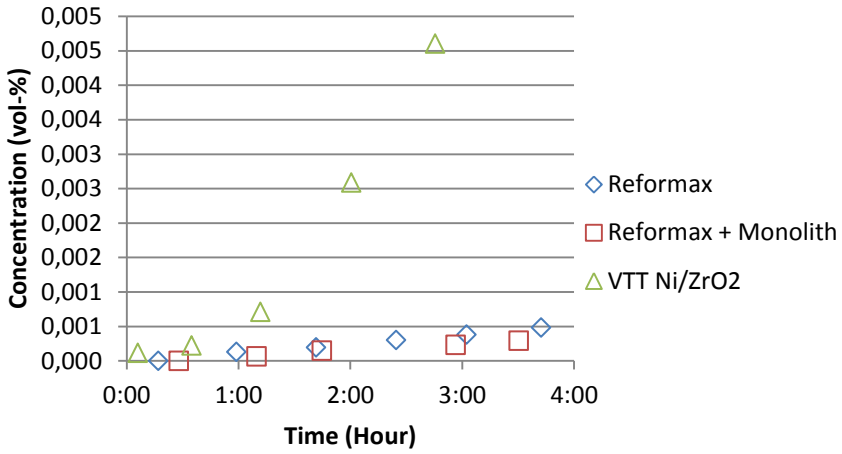

(a)

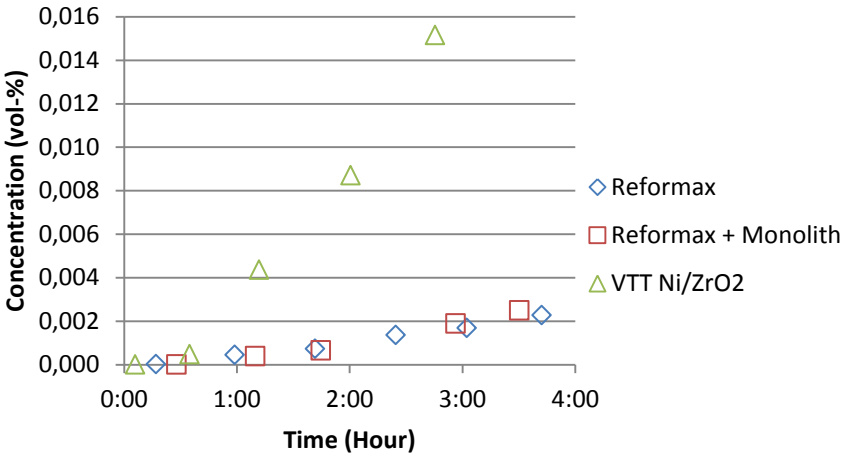

(b)

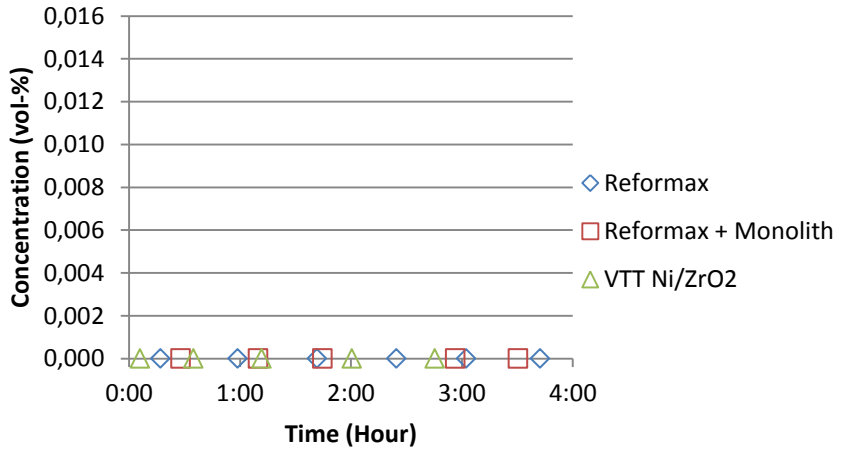

(c)

FIGURE 22 (a) Ethane (C_2H_6), (b) Ethene (C_2H_4) and (c) Ethyne (C_2H_2) production during steam reforming of pyrolysis oil aqueous fraction at 650°C, O/C ratio 0.95, using different catalysts and catalysts combinations

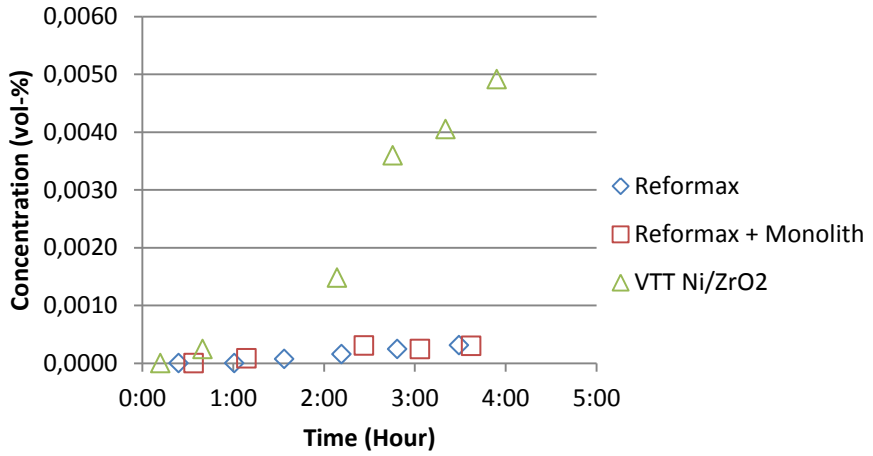

(a)

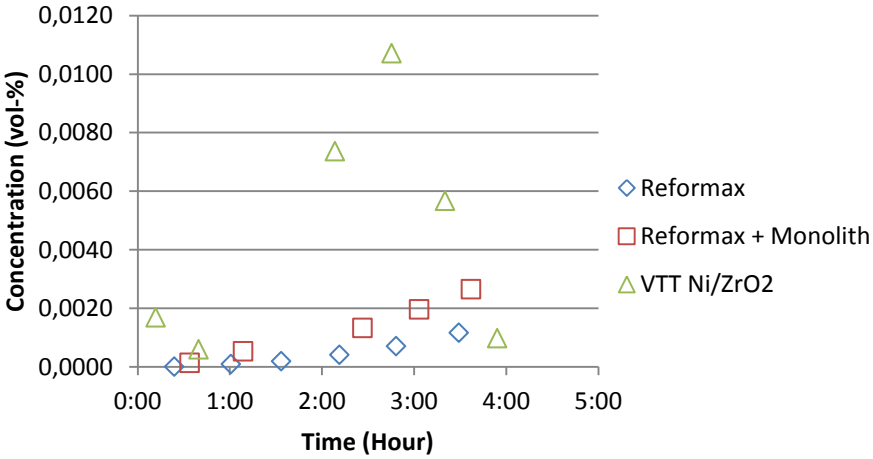

(b)

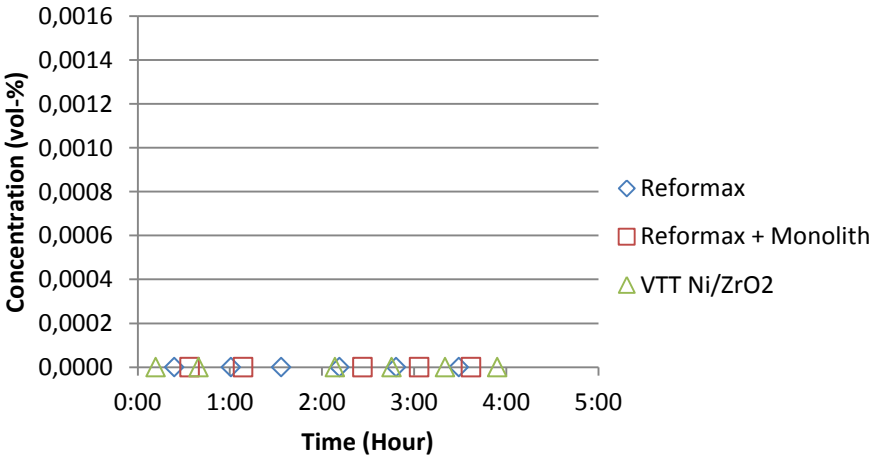

(c)

FIGURE 23 (a) Ethane (C_2H_6), (b) Ethene (C_2H_4) and (c) Ethyne (C_2H_2) production during steam reforming of pyrolysis oil aqueous fraction at 650°C, O/C ratio 1.1, using different catalysts and catalysts combinations